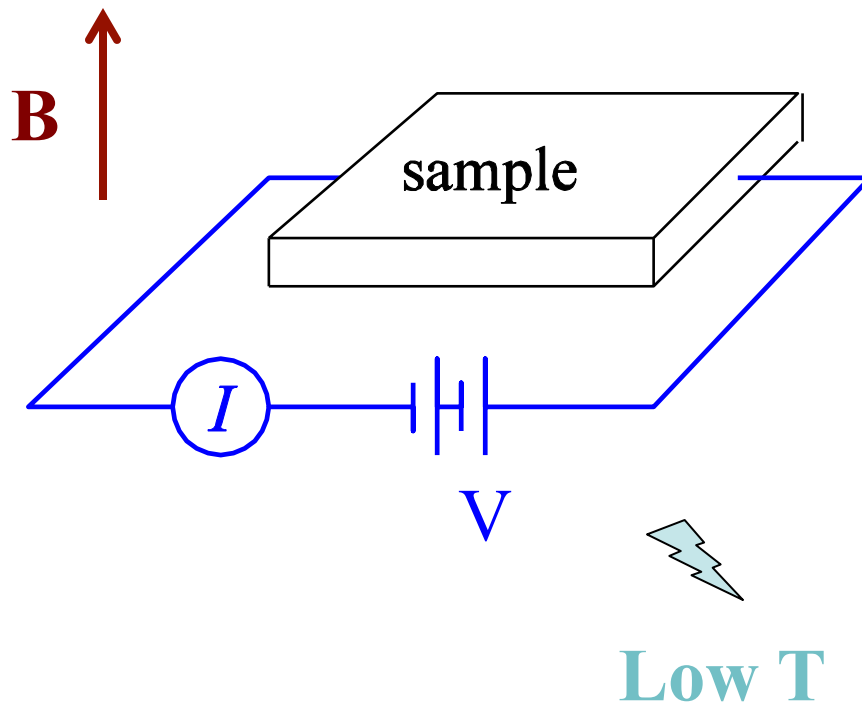


# Quantum transport in nanostructures

About the manifestations of quantum mechanics on the electrical transport properties of conductors



At macro scale

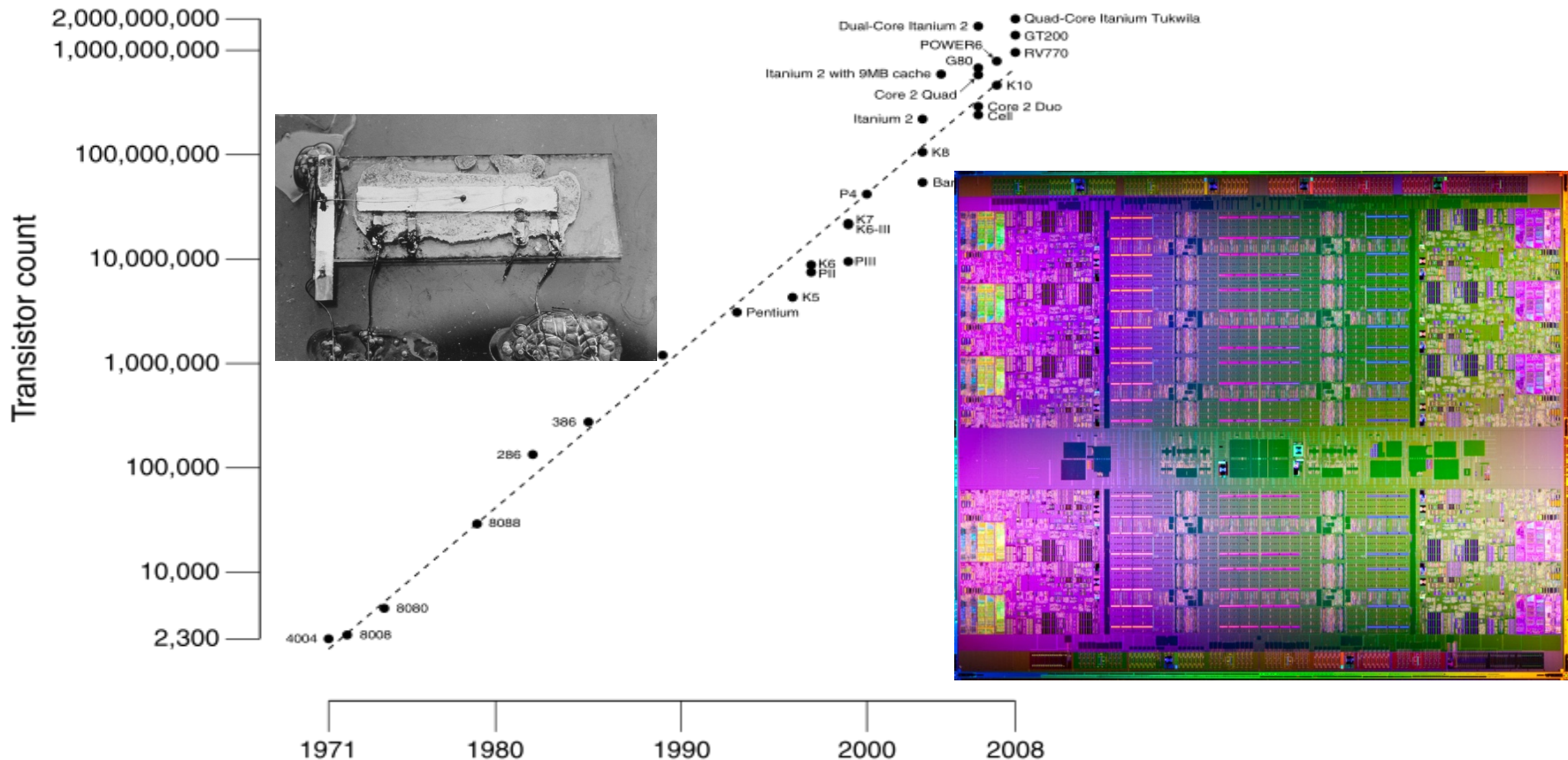
$$I = V/R \text{ (Ohm's law)}$$
$$= \sigma V$$

At nano scale

$$I \text{ ? } V$$

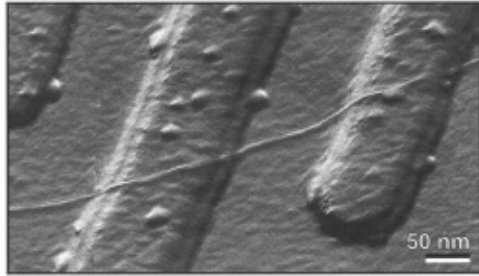
# Moore's Law

The number of transistors per microchip doubles roughly every two years.



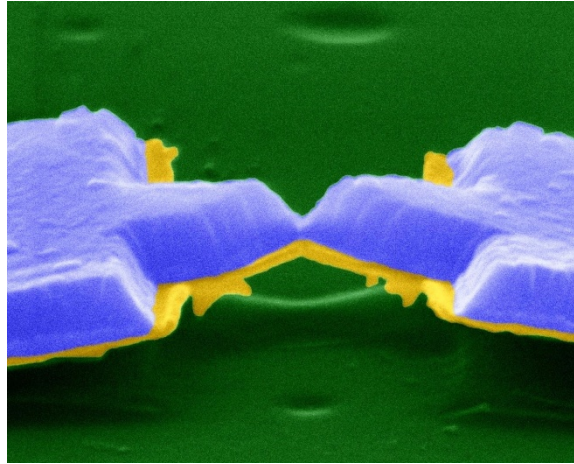
# Nanoscale electronics

## Nanotubes/wires



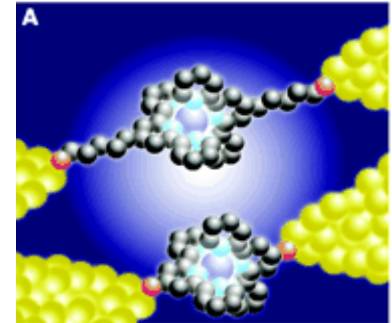
Tans *et al.* (1997)

## Atomic point contacts



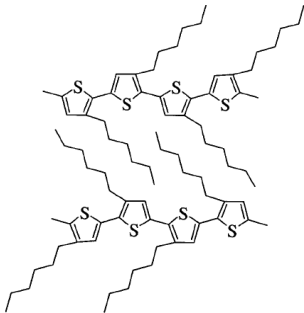
Scheer *et al.* (1998)

## Molecular junctions

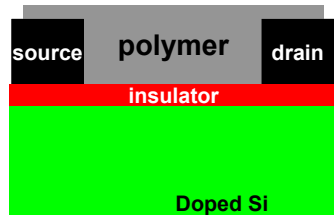


from Nitzan *et al.* (2003)

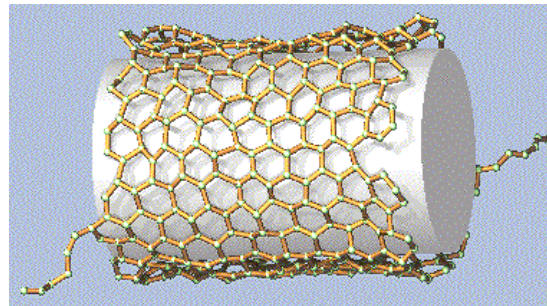
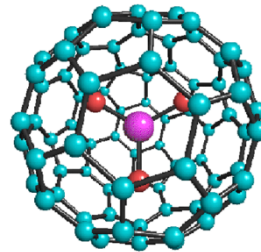
## Organic electronics



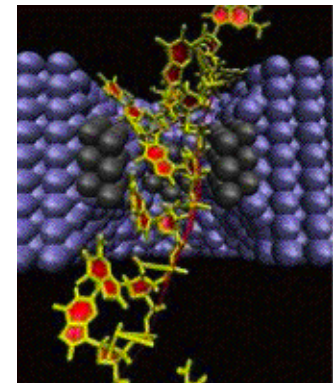
Poly(3-hexylthiophene)



Z.Q. Li *et al.* (2006)



## Fast DNA sequencing



Lagerqvist *et al.* (2006)

# Expected effects for electrons in nanostructures

- Quantum confinement effect
- Tunneling effects
- Charge discreteness and strong electron-electron Coulomb interaction effects
- Strong electric field effects
- Ballistic transport effects



# Important length scales

Elastic mean free path ( $l_e$ ): average distance the electrons travel without being elastically scattered

$$l_e = v_F \tau_e. \quad v_F \text{ denotes the Fermi velocity of the electrons}$$

Phase coherent length ( $l_\Phi$ ): average distance the electrons travel before their phase is randomized

$$l_\Phi = v_F \tau_\Phi. \quad \tau_\Phi \text{ denotes the dephasing time of the electrons}$$

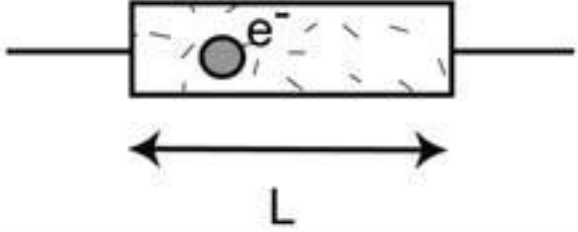
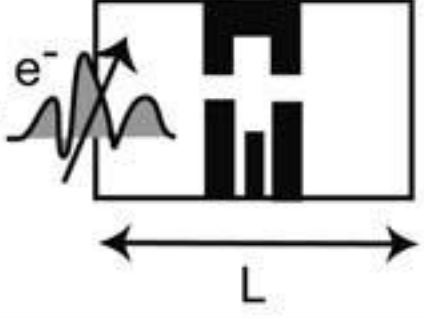
Fermi wavelength ( $\lambda_F$ ): de Broglie wavelength of Fermi electrons

$$\text{in } d = 3: \quad \lambda_F = 2^{3/2}(\pi/3n)^{1/3}$$

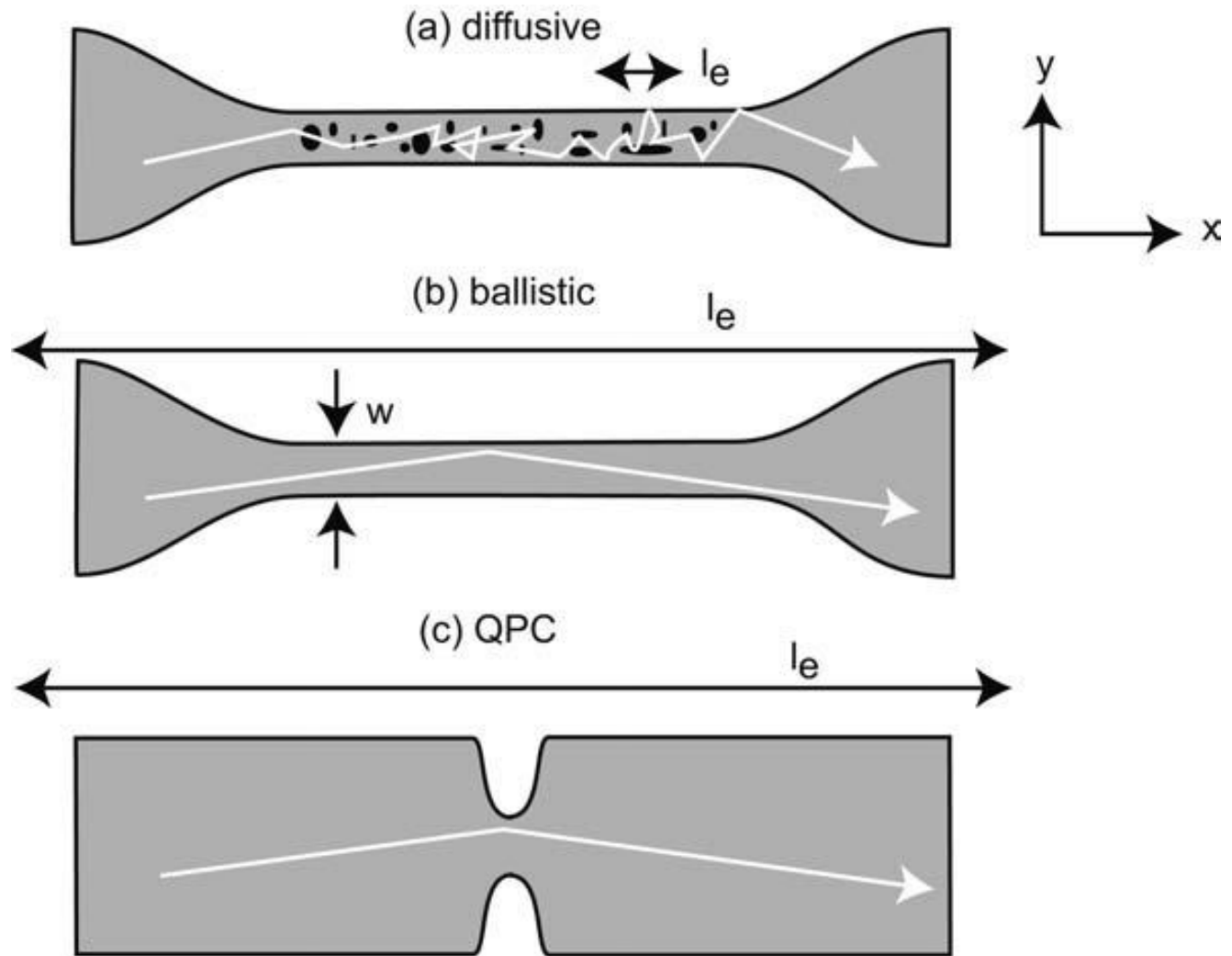
$$\text{in } d = 2: \quad \lambda_F = (2\pi/n)^{1/2}$$

$$\text{in } d = 1: \quad \lambda_F = 4/n$$

# Important mesoscopic regimes

<p>conventional device:</p> 	<p>mesoscopic device:</p> 
$L \gg l_e$ diffusive	$L \lesssim l_e$ ballistic
$L \gg l_\phi$ incoherent	$L \lesssim l_\phi$ phase coherent
$L \gg \lambda_F$ no size quantization	$L \lesssim \lambda_F$ size quantization
$e^2/C < k_B \Theta$ no single electron charging	$e^2/C \gtrsim k_B \Theta$ single electron charging effects
$L \gg l_s$ no spin effects	$L \lesssim l_s$ spin effects

# Quantum wires and point contact



# Typical length scale for mesoscopic regime

Temperature (K)	$L^*$ (nm)
4.2 (liquid helium)	$< 5000$
77 (liquid nitrogen)	$< 100$
300 (room temperature)	$< 10$

\*The numbers just give an order of magnitude

# Conduction at the macroscale

- Large number of states contribute to overall current
- Large number of electrons
- Resistivity, mobility, electric field, bias voltage, macroscopic currents are well-defined
- Quantum effects are averaged out by thermal effects



# Conduction at the nanoscale

- Small number of states can affect the overall current
- Wavefunction coherence lengths are comparable to characteristic device dimensions
- Single electrons charging effects can be significant
- These can amount to overall macroscopic electronic properties that show deviations from bulk electronic properties

# Boltzmann Transport Equation

Based on the semiclassical transport theory, considering the distributions of carriers to energies and momenta, taking into account scatterings.

The electrons obey the semiclassical equations of motion

$$\mathbf{v}(\mathbf{k}) = (1/\hbar)\nabla_{\mathbf{k}}\varepsilon(\mathbf{k})$$

$$d\mathbf{k}/dt = -e/\hbar (\mathbf{E} + \mathbf{v}(\mathbf{k}) \times \mathbf{B})$$

The general Boltzmann equation to first order approximation:

$$\mathbf{v}(\mathbf{k}) \cdot \nabla \varphi(\mathbf{k}, \mathbf{r}, t) - e\mathbf{E}/\hbar \cdot \nabla_{\mathbf{k}} \varphi(\mathbf{k}, \mathbf{r}, t) + \partial \varphi(\mathbf{k}, \mathbf{r}, t) / \partial t = [\partial \varphi(\mathbf{k}, \mathbf{r}, t) / \partial t]_{\text{scatter}}$$

Current density equals to the conductance times electric field

$$\mathbf{j} = \sigma \mathbf{E}$$

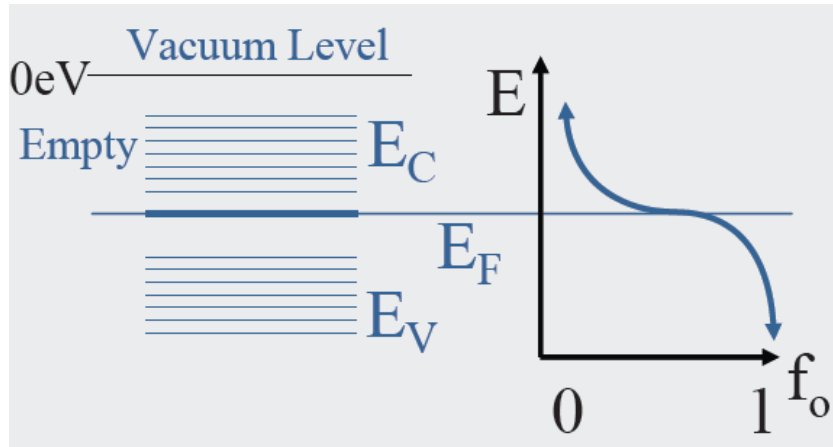
With simplified Boltzmann equation

$$\sigma = ne^2 \tau_D / m^* = ne \mu$$

the electron mobility  $\mu \equiv e \tau_D / m^*$ .

# Flow of electrons between two reservoirs

A metal/semiconductor electrode

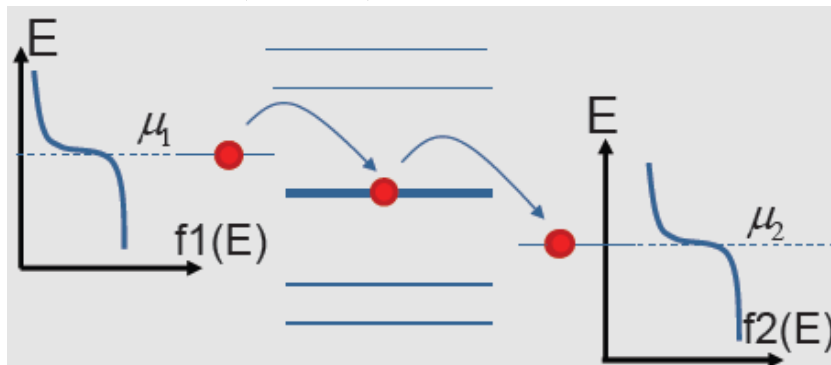


Electrons obey the Fermi-Dirac distribution

$$\bar{n}_i = \frac{1}{e^{(\epsilon_i - \mu)/kT} + 1}$$

As  $T \sim 0$  K, this is a step function

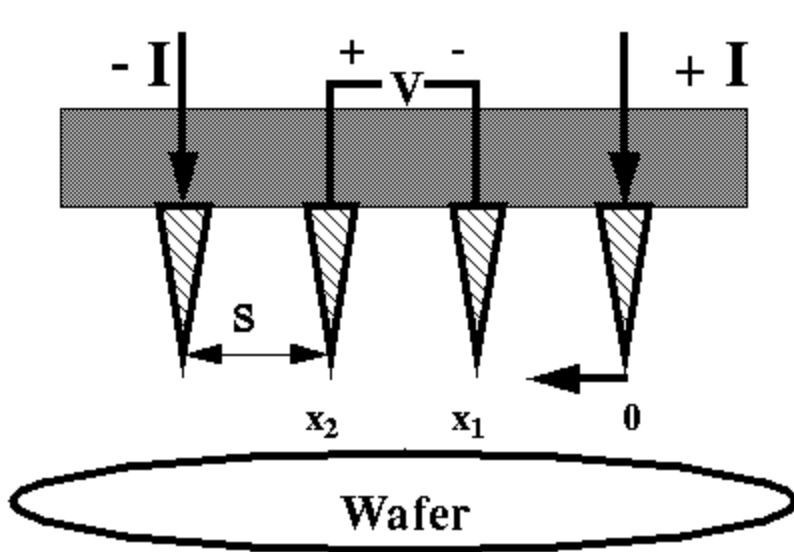
Two electrodes with some other material (states) in between



Availability of carriers on the left, and empty slots on the right, how fast the carriers tunnel from the left to the center and how fast the carriers tunnel from the center to the right basically determine the current.

# Four point technique

- Make quick measurements of conductivity on novel materials where contacts are not ideal



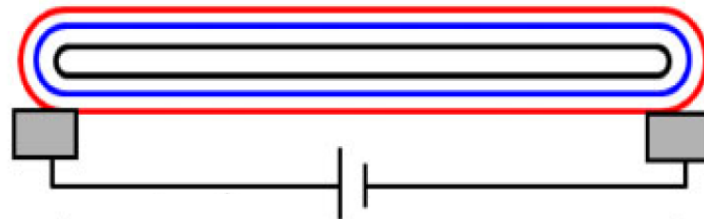
**Bulk Sample**  $\rho = 2\pi s \left( \frac{V}{I} \right)$   
 $t \gg s$

**Thin Sheet**  $\rho = \frac{\pi t}{\ln 2} \left( \frac{V}{I} \right)$   
thickness  $t \ll s$

Typical probe spacing  $s \sim 1 \text{ mm}$

# Electric Potential along Multiwall Carbon Nanotubes

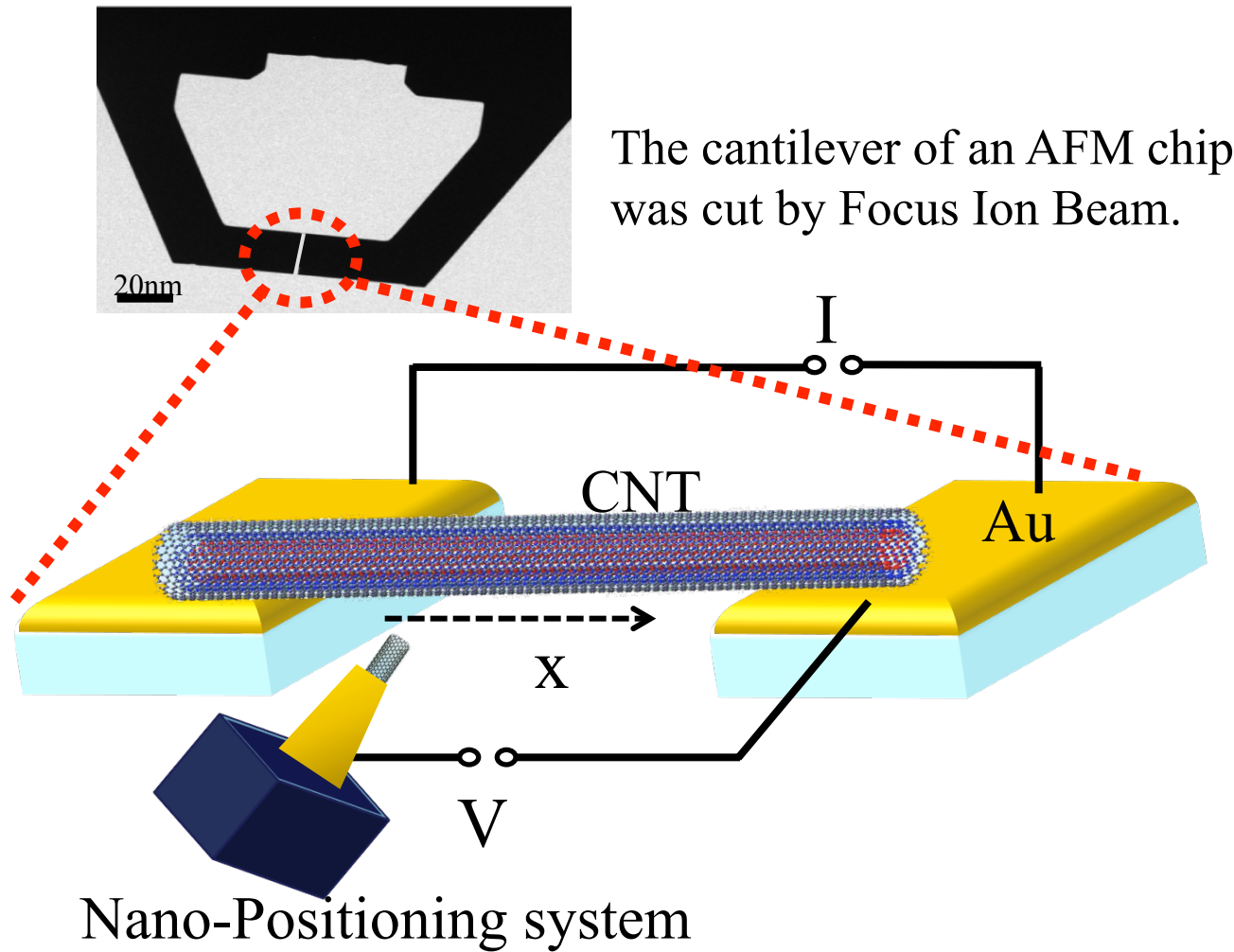
- For a side-bonded MWCNT, only the outermost shell is in direct contact with the electrodes.
- The intershell and intrashell current transport through a MWCNT is of great concerns.
- A MWCNT was electrically breakdown into several sections.
- The electrical properties of a MWCNT with different sections is observed.



A side-bonded nanotube



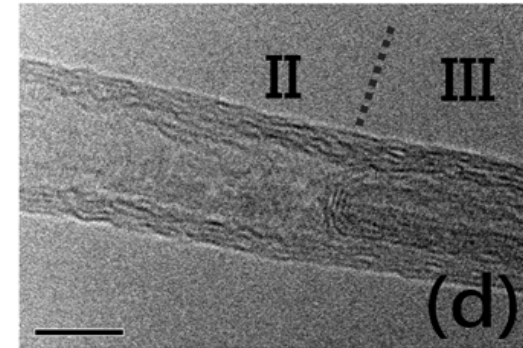
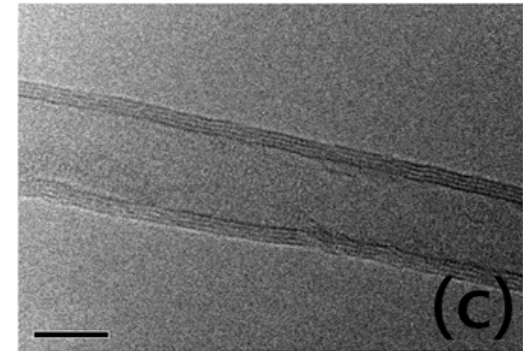
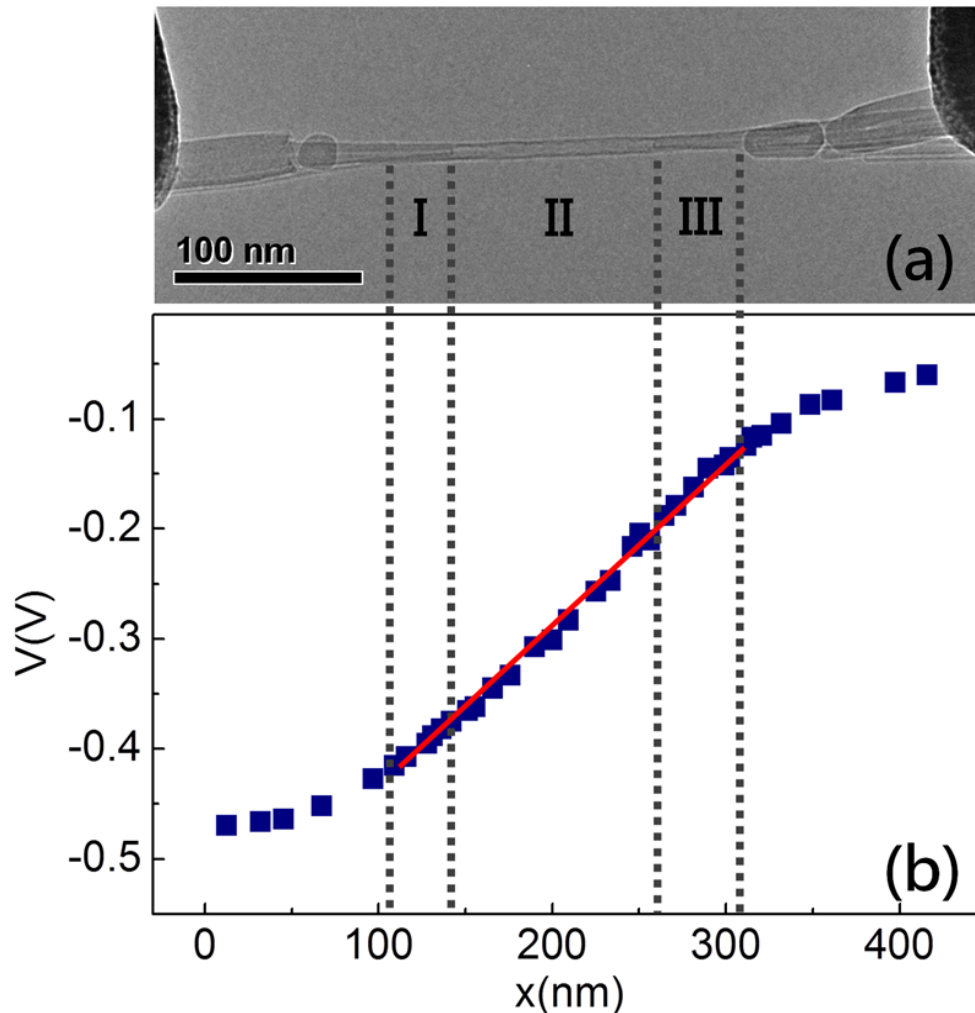
# *Experimental*





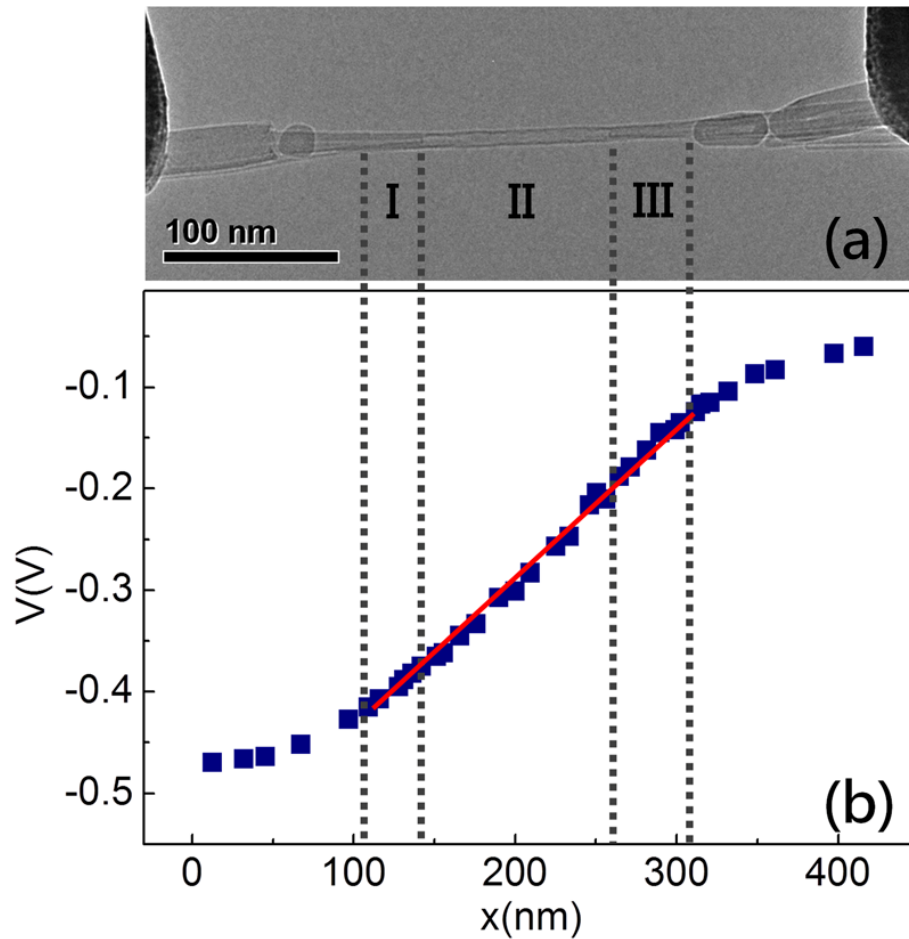
Movie: Probing the potential along a MWCNT

# Results and Discussion



The slope of the voltage drop does not change at I, II and III sections.

- (a) TEM image of a MWCNT. Three distinct sections are shown with the same outermost shell.
- (b) The measured potential profile along the MWCNT at a constant current of  $10\mu A$ .
- (c) There are four shells at section II. Scale bar: 5 nm.
- (d) TEM image at the interface between section II and III. Scale bar: 5 nm.



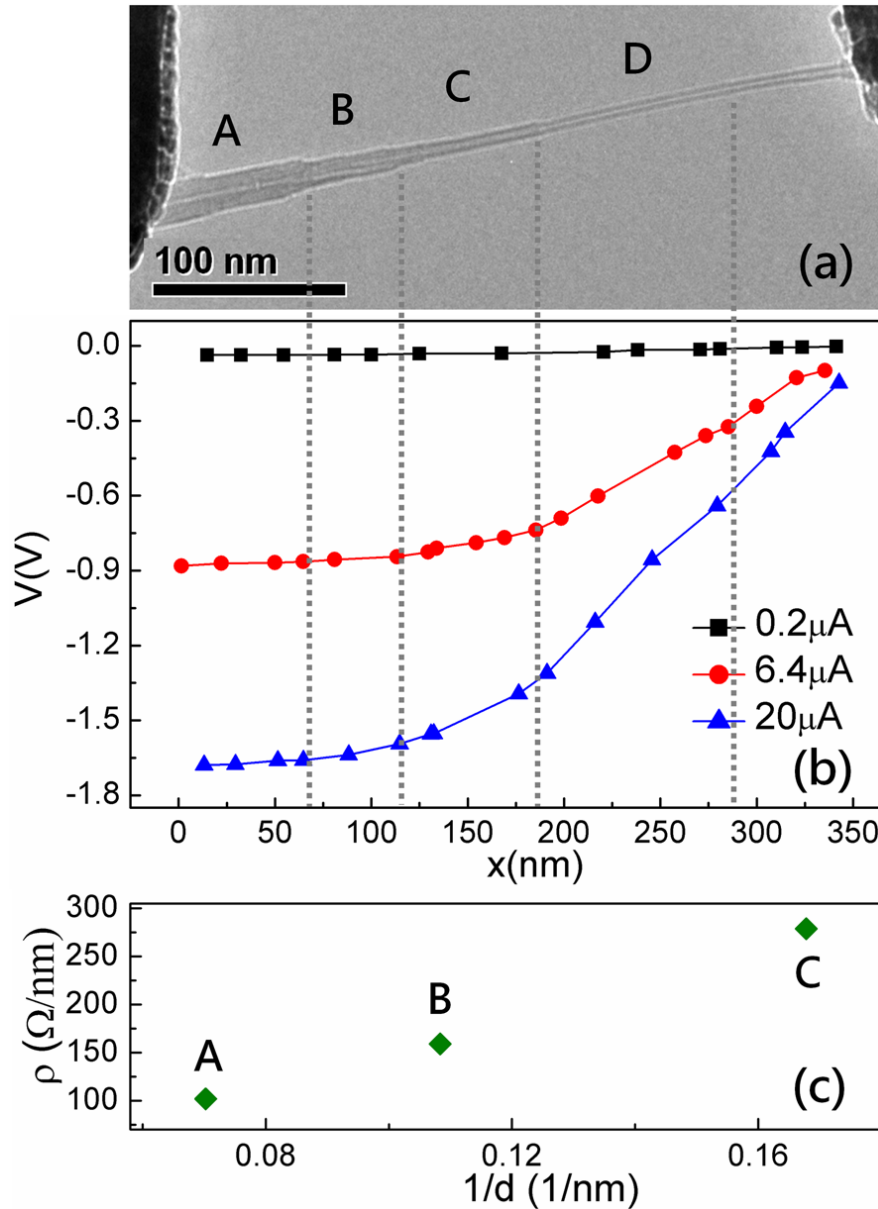
The slope of the voltage drop:

$$\frac{dV(x)}{dx} = -\rho_1 I_1(x)$$

$\rho_1$  : intrashell resistance per unit  
length of the outermost shell  
 $I_1$  : current on the outermost shell

$\rho_1$  at sections I, II, and III  
are the same.

*→ the same current on  
the outermost  
shell of section I, II,  
and III.*

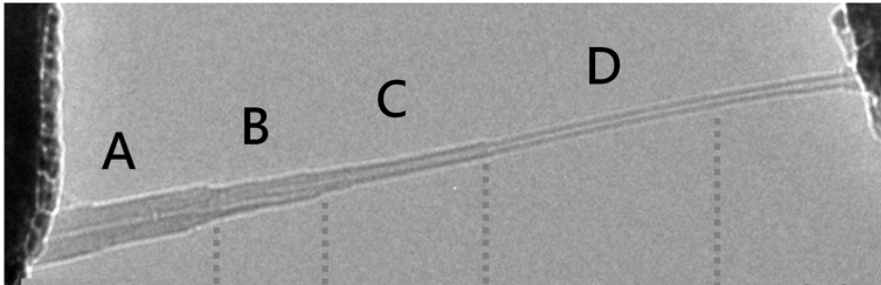


At small current ( $0.2 \mu A$ ), the current mainly flows on the outermost shell of the nanotube.

→ The resistance per nanometer of the outermost shell  $\rho$  ( $\Omega/nm$ ) is obtained:

$$\rho = -31.65 + \frac{1833}{d}$$

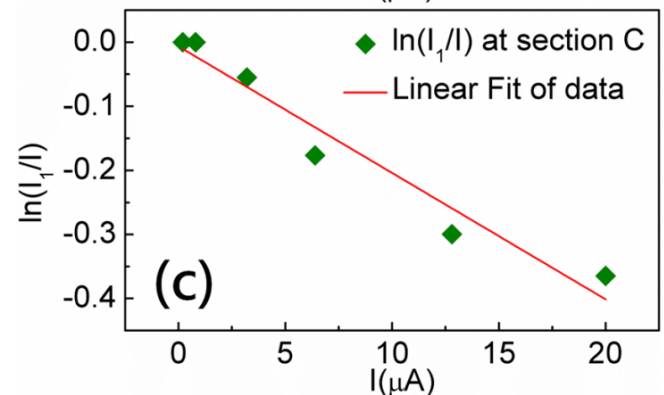
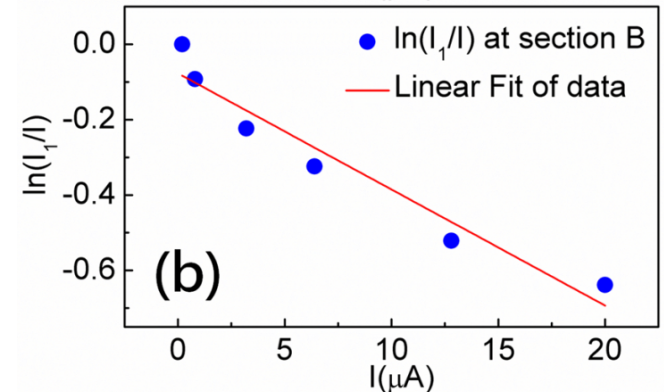
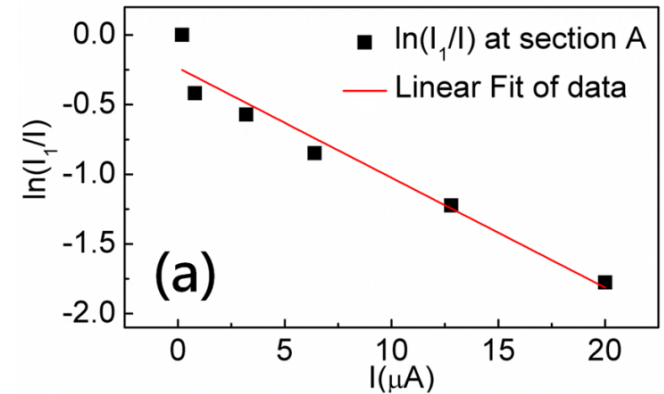


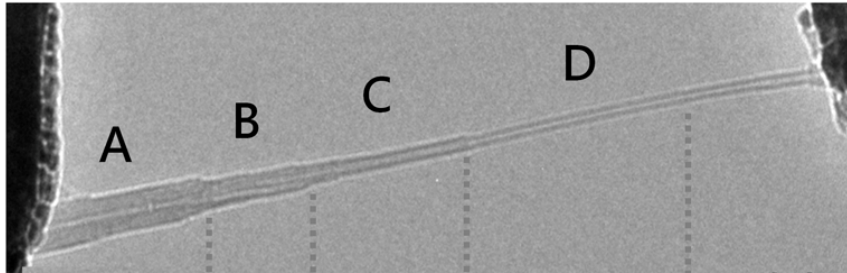


When the total current was larger,  
more proportion of the total  
current hopped into the inner  
shells:

$$\frac{I_1}{I} = e^{-\frac{I}{I_C(d)}}$$

Intershell coupling is energy dependent



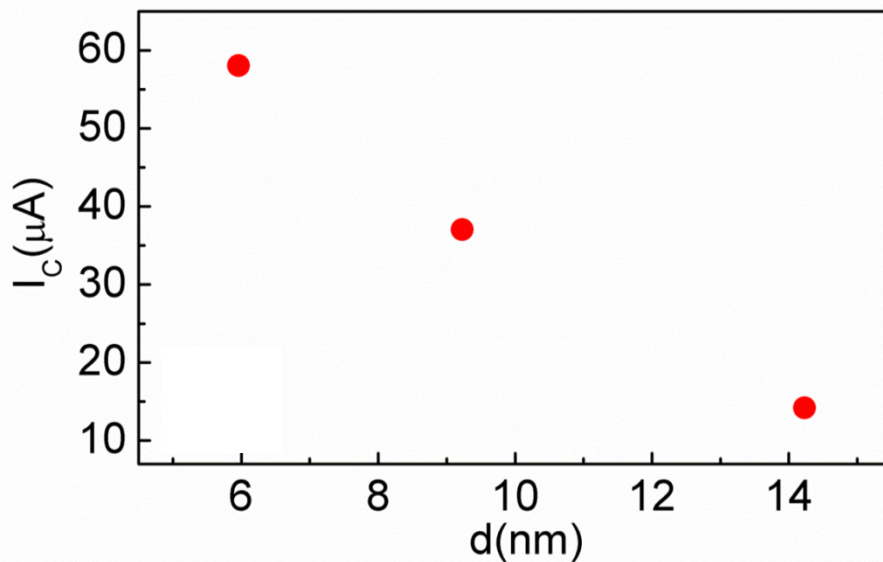


$$\frac{I_1}{I} = e^{-\frac{I}{I_C(d)}}$$

$$(I_C = 76.48 - 4.54d)$$

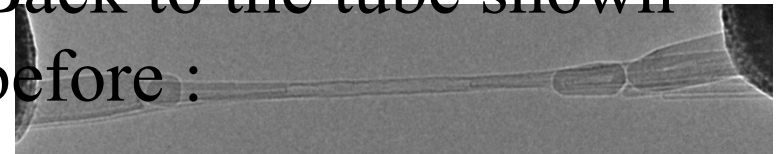
$$I_1 = I e^{-\frac{I}{I_C(d_1)}}$$

$$I_2 = (I - I_1) e^{-\frac{I - I_1}{I_C(d_2)}}$$



The value of  $I_c$  is also diameter dependent

Back to the tube shown before :



when the total current is 10 μA:

$$I_1 = 7.8 \mu A$$

$$I_2 = 2.1 \mu A$$

99% of the total current was distributed on the outer two shells!

2-D nanostructures:

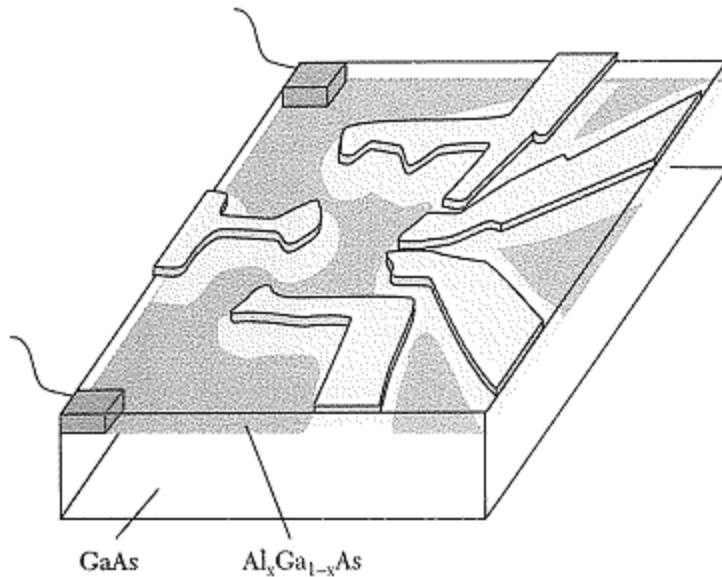
graphene, metallic thin films, superlattices, ... .

1-D nanostructures:

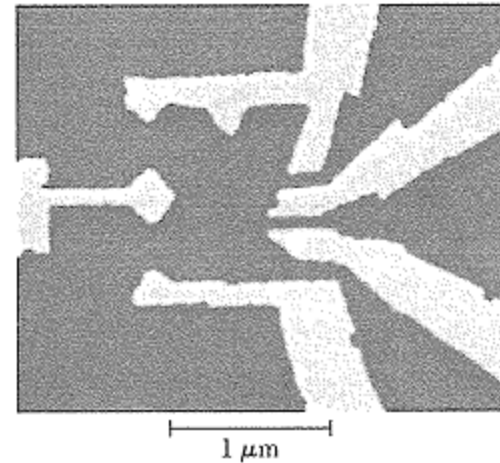
carbon nanotubes, quantum wires, conducting polymers, ... .

0-D nanostructures:

semiconductor nanocrystals, metal nanoparticles,  
lithographically patterned quantum dots, ... .

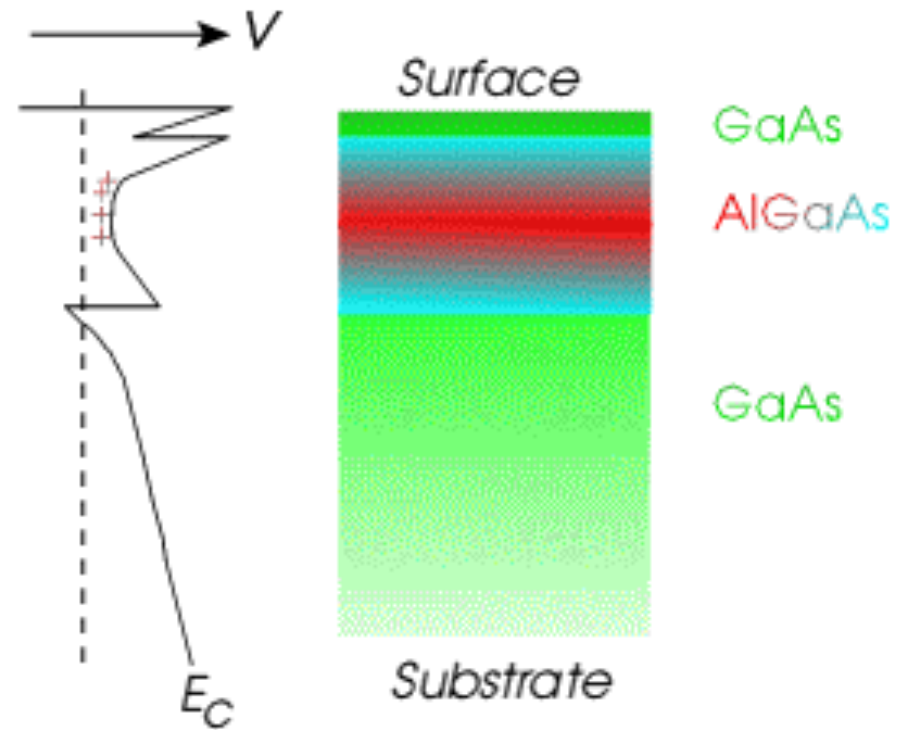
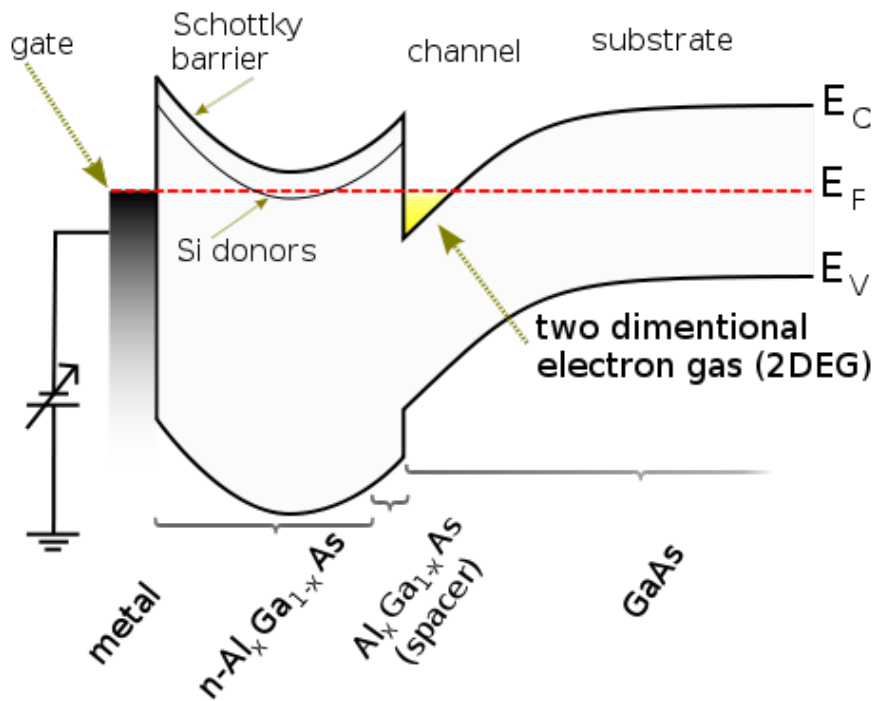


Gate electrode pattern of  
a quantum dot on 2DEG

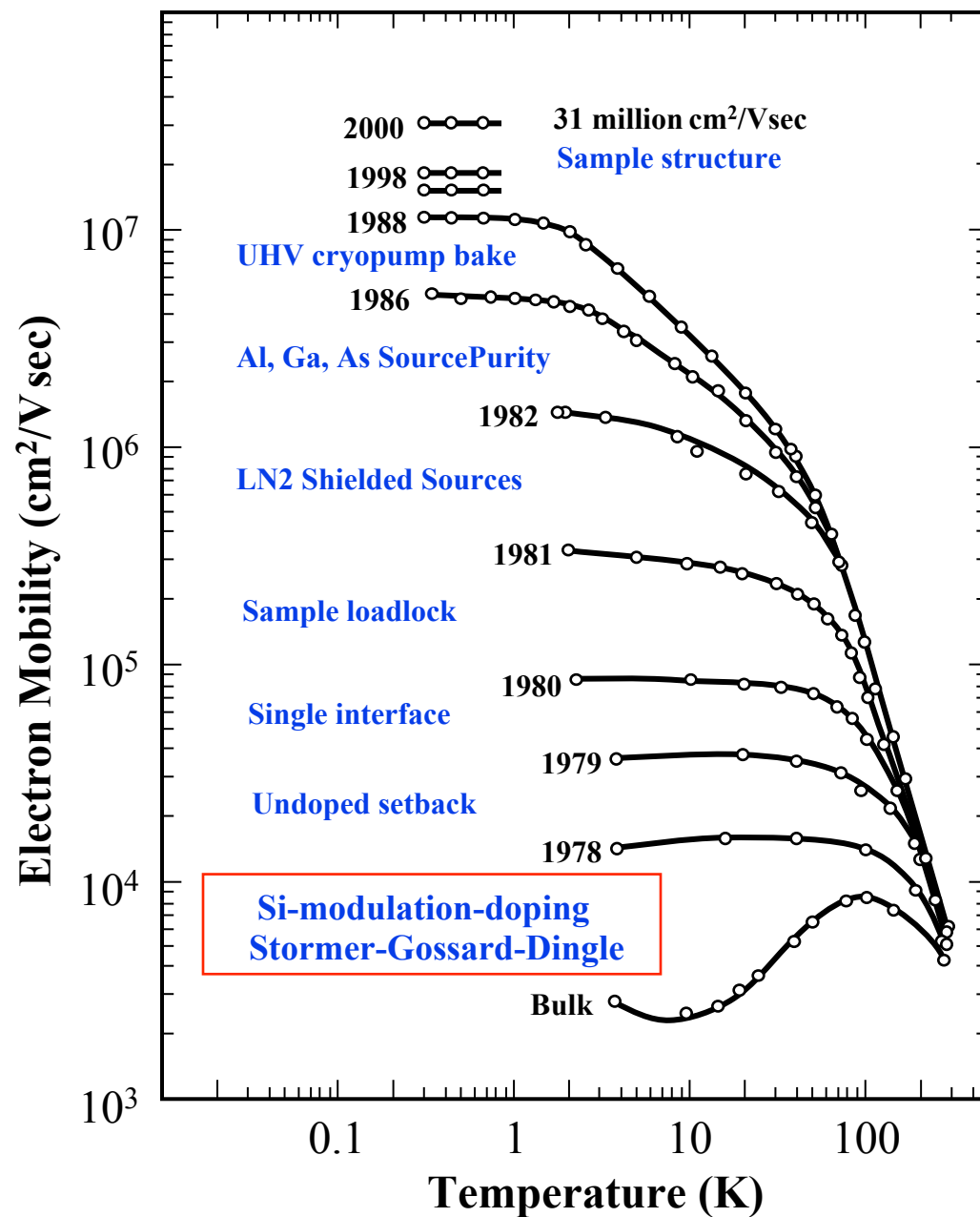


SEM image

# 2D electron gas (2DEG)



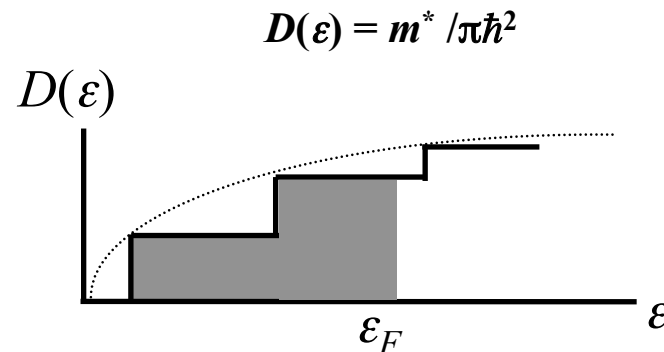
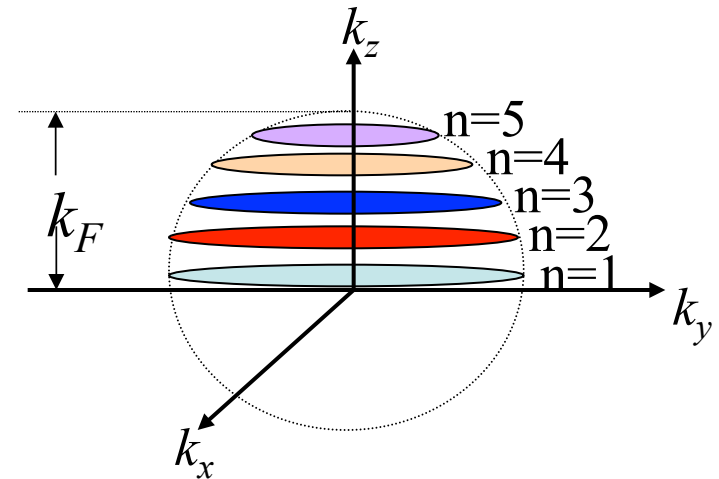
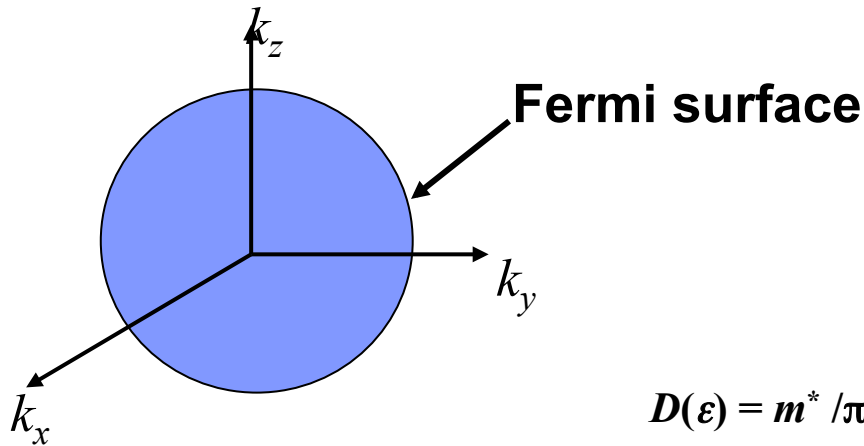
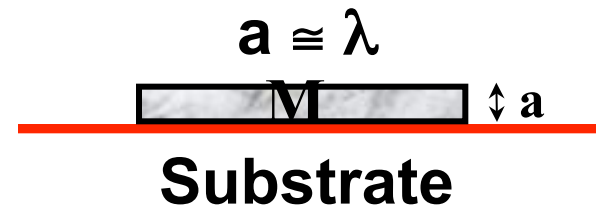
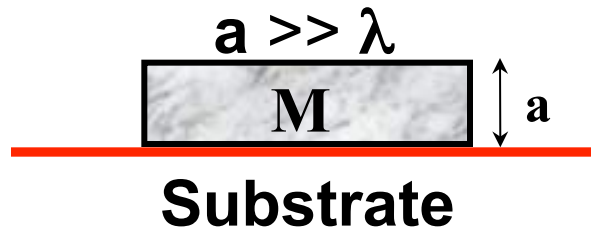
# Historical landmarks of 2DEG mobility in GaAs.



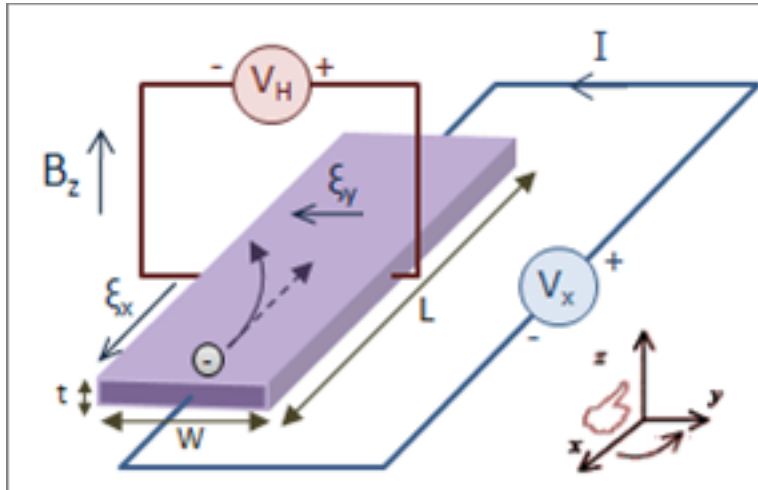
# Electronic Structure of 2-D Systems

$\lambda$  = de Broglie wavelength of electron

$a$  = thickness of metal film



# Classical Hall effect (1880 E.H. Hall)



Lorentz-force on electron:

$$m\dot{\vec{v}} = -e(\vec{E} + \vec{v} \times \vec{B}) = 0 \quad \Rightarrow \quad \vec{E} = -\vec{v} \times \vec{B}$$

stationary current:

$$\vec{j} = -e\rho \vec{v}$$

$$j_x = \frac{e\rho}{B} E_y \quad j_y = \frac{e\rho}{B} E_x$$

Hall resistance:

$$R_{xy} = E_y/(j_x B) = 1/\rho e$$

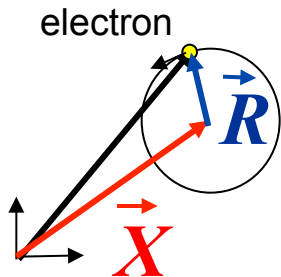
# 2D electrons in magnetic fields: Landau levels

**Hamiltonian:**  $H = \frac{1}{2m} \left[ (p_x + eA_x)^2 + (p_y + eA_y)^2 \right]$

coordinate transformation:

$$(x, p_x) \quad (y, p_y) \quad \longrightarrow \quad (X, Y) \quad (R_x, R_y)$$

center of  
cyclotron motion      radial vector of  
cyclotron motion



$$X = x - R_x$$

$$Y = y - R_y$$

$$R_x = -\frac{p_y + eA_y}{eB}$$

$$R_y = \frac{p_x + eA_x}{eB}$$

commutation relations:

$$[X, R_x] = [X, R_y] = [Y, R_x] = [Y, R_y] = 0$$

$$[X, Y] = -il_m^2$$

$$[R_x, R_y] = -il_m^2$$

$$l_m \equiv \sqrt{\frac{\hbar}{eB}}$$



# 2D electrons in magnetic fields: Landau levels

mapping to oscillator:

$$\hat{a} = \frac{1}{\sqrt{2}l_m} (R_y - iR_x) \quad \hat{b} = \frac{1}{\sqrt{2}l_m} (X - iY)$$

$$[\hat{a}, \hat{a}^\dagger] = 1 \quad [\hat{b}, \hat{b}^\dagger] = 1$$

$$H = \hbar\omega_c R^2 / 2 l_m^2 = \hbar\omega_c (a^+ a + 1/2)$$

**Landau levels**

# 2D electrons in magnetic fields: Landau levels

## typical scales:

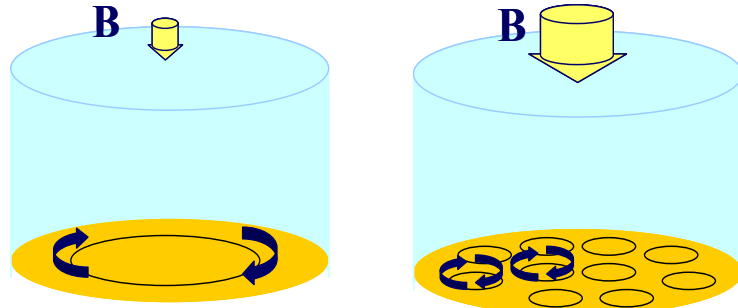
- length

$$\langle R^2 \rangle_n = (1 + 2n) l_m^2$$

$$l_m \equiv \sqrt{\frac{\hbar}{eB}}$$

- energy

$$\hbar\omega_c = \frac{\hbar eB}{m} = \frac{l_m^2}{m}$$



**magnetic length**

**cyclotron frequency**

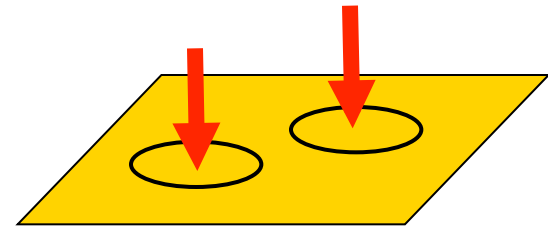
# 2D electrons in magnetic fields: Landau levels

## degeneracy of Landau levels:

center of cyclotron motion  $(X, Y)$  arbitrary  $\rightarrow$   
degeneracy

- **2D density of states (DOS)**

$$\varrho_{\text{DS}} = \frac{1}{2\pi l_m^2} = \frac{eB}{2\pi\hbar} = \frac{B}{\Phi_D}$$



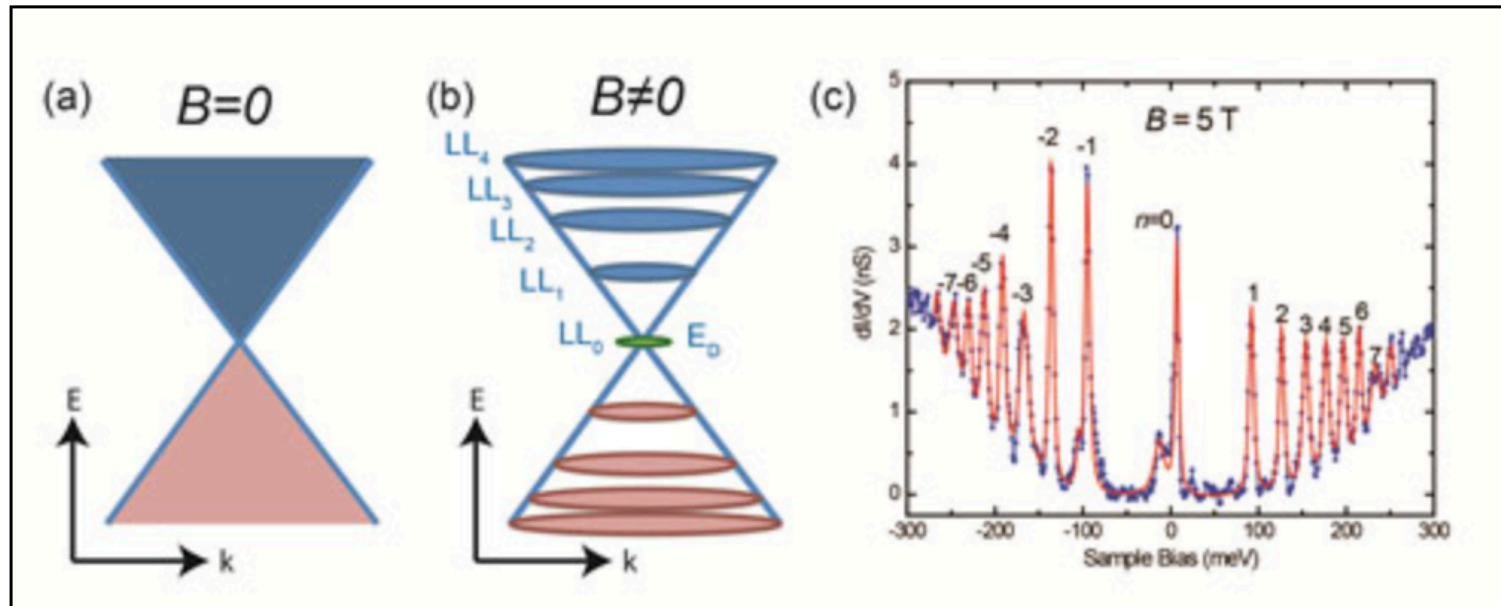
one state per area of cyclotron orbit

- **filling factor**

$$\nu = \frac{\varrho}{\varrho_{\text{DS}}} = 2\pi l_m^2 \varrho = \frac{\rho \Phi_D}{B} = \frac{N}{N_\Phi}$$

# atoms / # flux quanta

# Landau levels in Graphene



*Conduction (blue) and valence (pink) bands meet at a conical point with a linear energy-momentum dispersion for graphene. (b) The graphene carriers condense into narrow energy levels (Landau levels) when placed in a perpendicular magnetic field,  $B$ . (c) Direct measurement of graphene Landau levels with high resolution scanning tunneling spectroscopy.*

D. L. Miller, K. D. Kubista, G. M. Rutter, M. Ruan, W. A. deHeer, P. N. First, and J. A. Stroscio, *Science* **324**, 924-927 (2009).

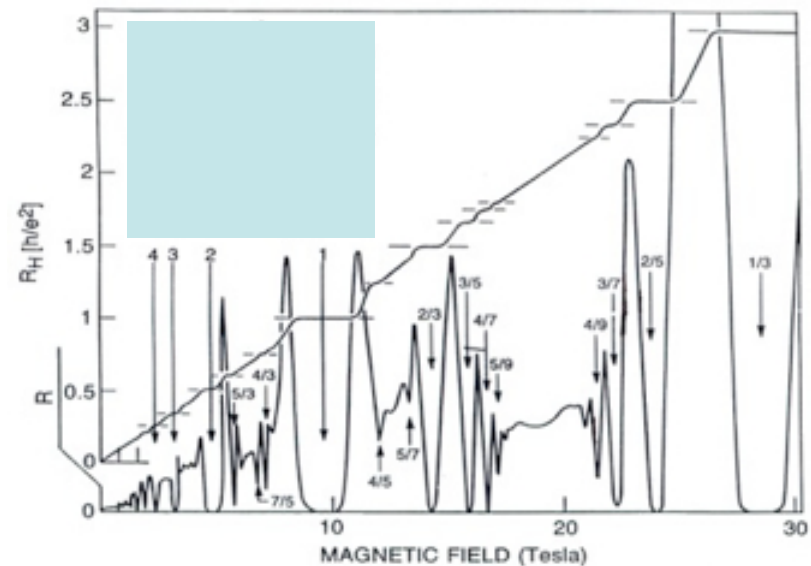
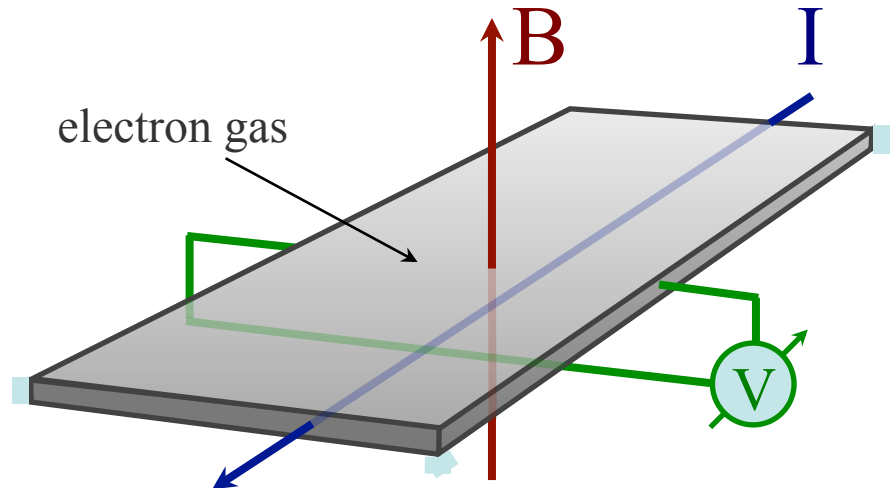
# Quantum Hall effect

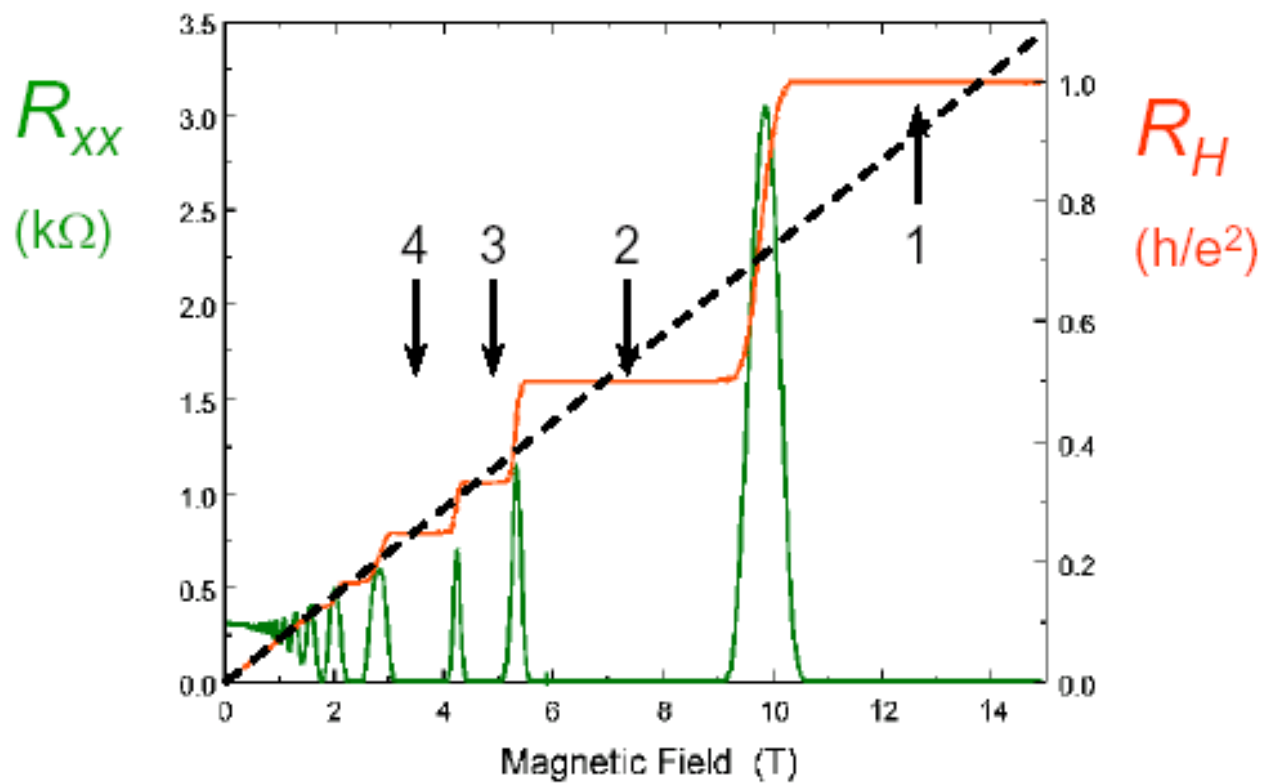
Quantization of conductivity  
for a two-dimensional electron gas  
at very low temperatures  
in a high magnetic field.

$$\sigma = \nu \frac{e^2}{h}$$



Semiconductor heterostructure confines  
electron gas to two spatial dimensions.



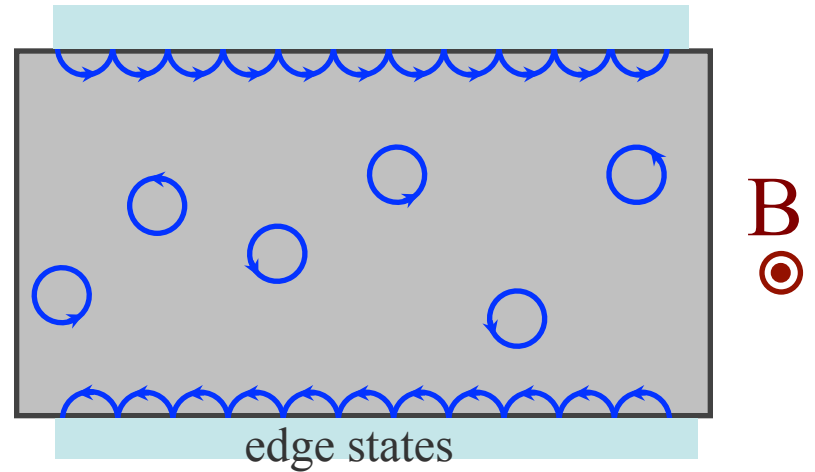


$$R_H = (1/\nu)(h/e^2)$$

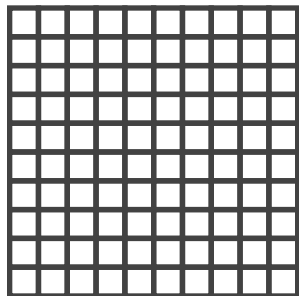
# Quantum Hall states

Landau levels

$$E_n = h \frac{eB}{m} \left( n + \frac{1}{2} \right)$$



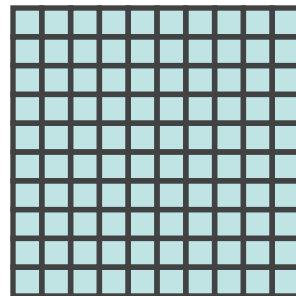
Landau level degeneracy



$$2\Phi/\Phi_0$$

orbital states

integer quantum Hall

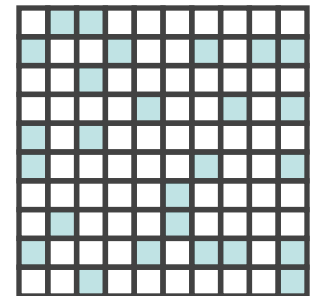


filled level



incompressible liquid

fractional quantum Hall



partially filled level



Coulomb repulsion

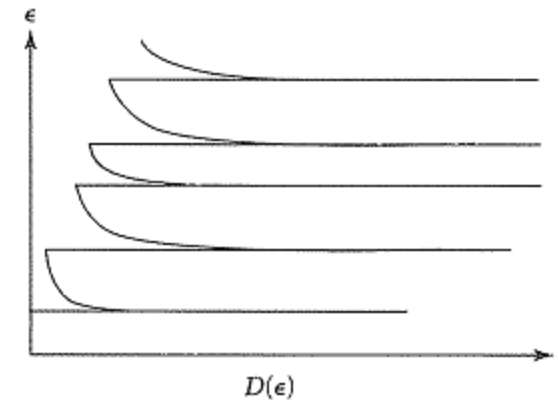
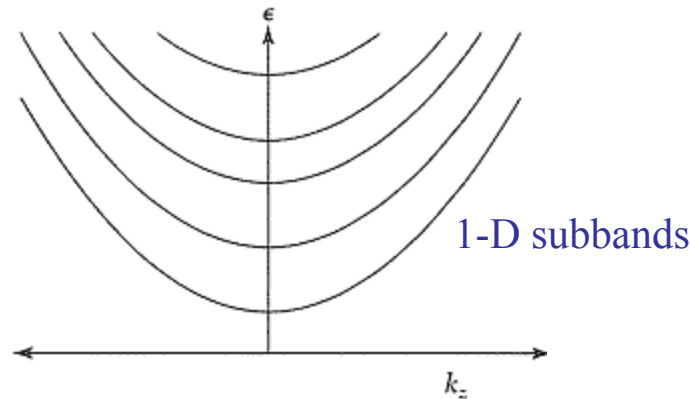
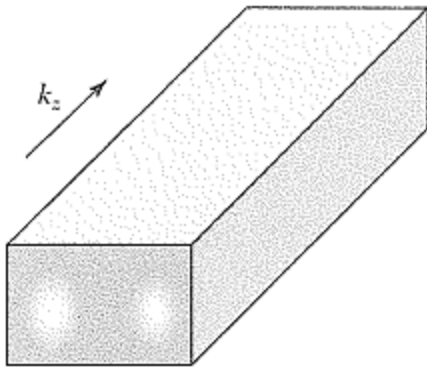
incompressible liquid

# Electronic Structure of 1-D Systems

$$\epsilon = \epsilon_{i,j} + \frac{\hbar^2 k^2}{2m}$$

$$\psi(x, y, z) = \psi_{i,j}(x, y) e^{ikz}$$

$i, j$  = quantum numbers in the cross section



$$D(\epsilon) = \sum_{i,j} D_{i,j}(\epsilon) \quad D_{i,j}(\epsilon) = \frac{dN_{i,j}}{dk} \frac{dk}{d\epsilon} = 2 \times 2 \frac{L}{2\pi} \sqrt{\frac{m}{2\hbar^2(\epsilon - \epsilon_{i,j})}} = \begin{cases} \frac{4L}{\hbar v_{i,j}} & \epsilon > \epsilon_{i,j} \\ 0 & \epsilon < \epsilon_{i,j} \end{cases}$$

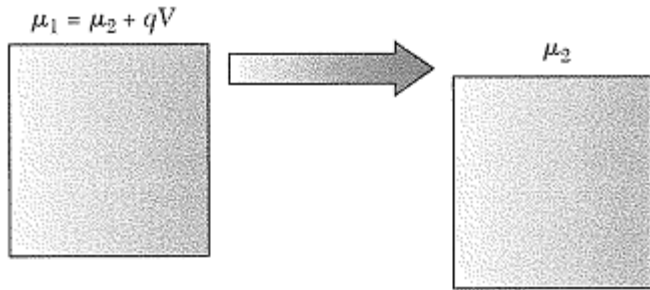
Let there be  $n_{1D}$  carriers per unit length, then 
$$n_{1D} = \frac{2}{2\pi} 2k_F = \frac{2}{\pi} k_F$$

Fermi surface consists of 2 points at  $k = \pm k_F$

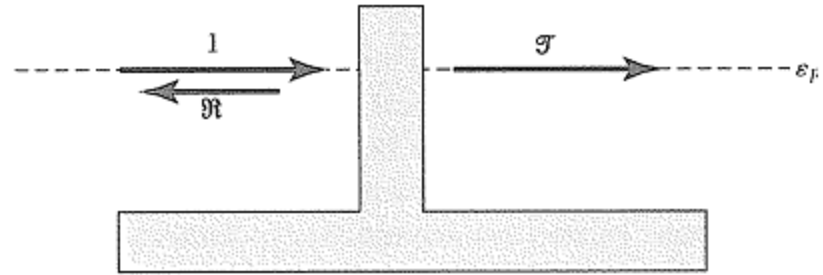


# Electrical Transport in 1-D

## Conductance Quantization & the Landauer Formula



1-D channel with 1 occupied subband connecting 2 large reservoir.



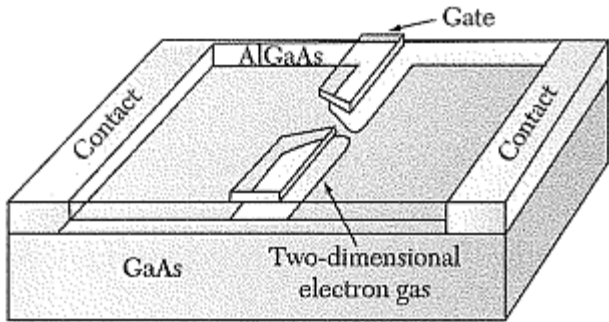
Barrier model for imperfect 1-D channel

Let  $\Delta n$  be the excess right-moving carrier density,  $D_R(\epsilon)$  be the corresponding DOS.

$$I = \Delta n q v = \frac{D_R(\epsilon) q V}{L} q v = \frac{2}{h v} q^2 V v = \frac{2 e^2}{h} V \quad q = \pm e$$

→ The **conductance quantum**  $G_Q = \frac{2 e^2}{h}$  depends only on fundamental constants.

Likewise the **resistance quantum**  $R_Q = \frac{1}{G_Q} = \frac{h}{2 e^2}$



If channel is not perfectly conducting,

$$G(\varepsilon_F) = \frac{2e^2}{h} \mathcal{T}(\varepsilon_F) \quad \text{Landauer formula}$$

$\mathcal{T}$  = transmission coefficient.

For multi-channel quasi-1-D systems

$$\mathcal{T}(\varepsilon_F) = \sum_{i,j} \mathcal{T}_{i,j}(\varepsilon_F)$$

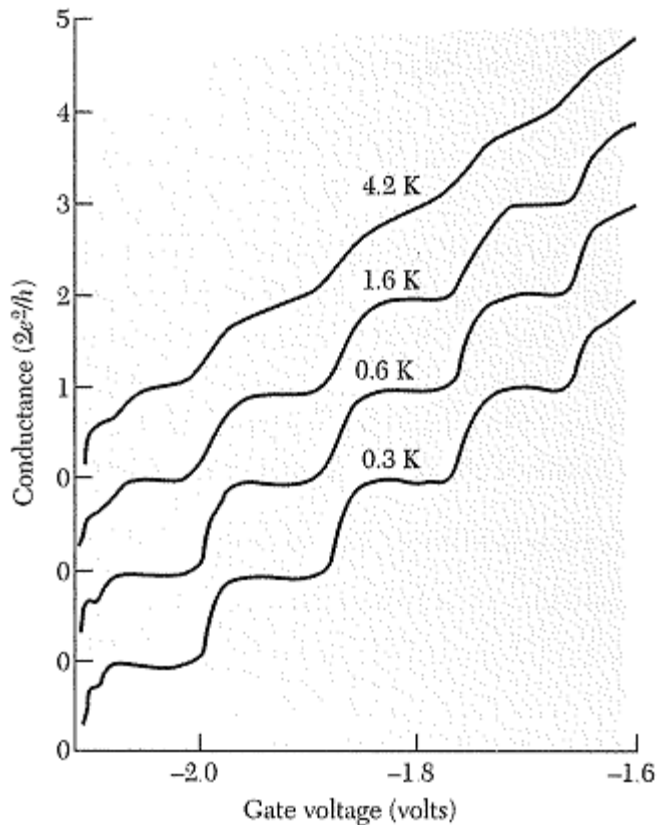
$i, j$  label transverse eigenstates.

For finite  $T$ ,

$$I(\varepsilon_F, V, T) = \frac{2e^2}{h} \int_{-\infty}^{\infty} d\varepsilon [f_L(\varepsilon - eV) - f_R(\varepsilon)] \mathcal{T}(\varepsilon)$$

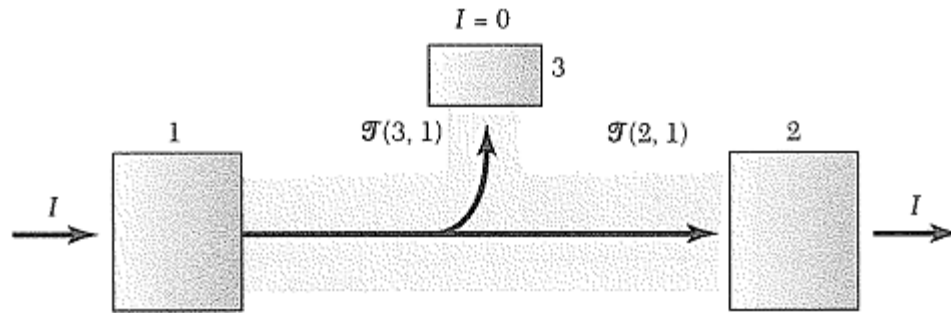
$$R = \frac{h}{2e^2 \mathcal{T}} = \frac{h}{2e^2} \frac{\mathcal{T} + (1 - \mathcal{T})}{\mathcal{T}} = \frac{h}{2e^2} + \frac{h}{2e^2} \frac{R}{\mathcal{T}}$$

$R$  = reflection coefficient.



Channel fully depleted of carriers at  $V_g = -2.1$  V.

# Voltage Probes & the Buttiker-Landauer Formulism



$\mathcal{T}^{(n,m)}$  = total transmission probability for an  $e$  to go from  $m$  to  $n$  contact.

1,2 are current probes; 3 is voltage probe.

For a current probe  $n$  with  $N$  channels,  $\mu$  of contact is fixed by  $V$ .

Net current thru contact is 
$$I_n = \frac{2e^2}{h} \left( N_n V_n - \sum_m \mathcal{T}^{(n,m)} V_m \right)$$

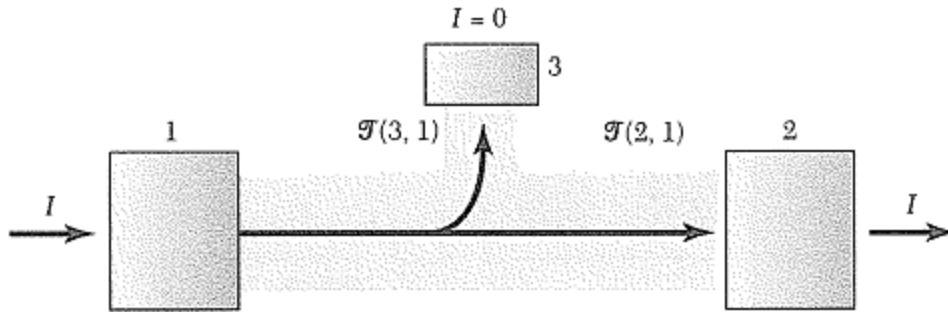
Setting  $I_n = 0$ ,  $V_n = V \quad \forall n \quad \rightarrow \quad N_n = \sum_m \mathcal{T}^{(n,m)}$

For the voltage probe  $n$ ,  $V_n$  adjusts itself so that  $I_n = 0$ .

$$\rightarrow V_n = \frac{1}{N_n} \sum_m \mathcal{T}^{(n,m)} V_m = \frac{\sum_m \mathcal{T}^{(n,m)} V_m}{\sum_m \mathcal{T}^{(n,m)}} \quad \mu_n = \frac{\sum_m \mathcal{T}^{(n,m)} \mu_m}{\sum_m \mathcal{T}^{(n,m)}}$$

$I_n, V_n$  depend on  $T^{(n,m)} \rightarrow$  their values are path dependent.

Voltage probe can disturb existent paths.



Let every  $e$  leaving 1 always arrive either at 2 or 3 with no back scattering.

$$V_3 = \frac{T^{(3,1)} V}{T^{(3,1)} + T^{(3,2)}} = \frac{V}{2} \quad \text{if } T^{(3,1)} = T^{(3,2)}$$

Current out of 1: 
$$I = \frac{2e^2}{h} \left( V - T^{(1,3)} V_3 \right) = \frac{2e^2}{h} V \left( 1 - \frac{1}{2} T^{(1,3)} \right) < \frac{2e^2}{h} V \quad \text{no probe}$$

# Conductance of a quantum point contact

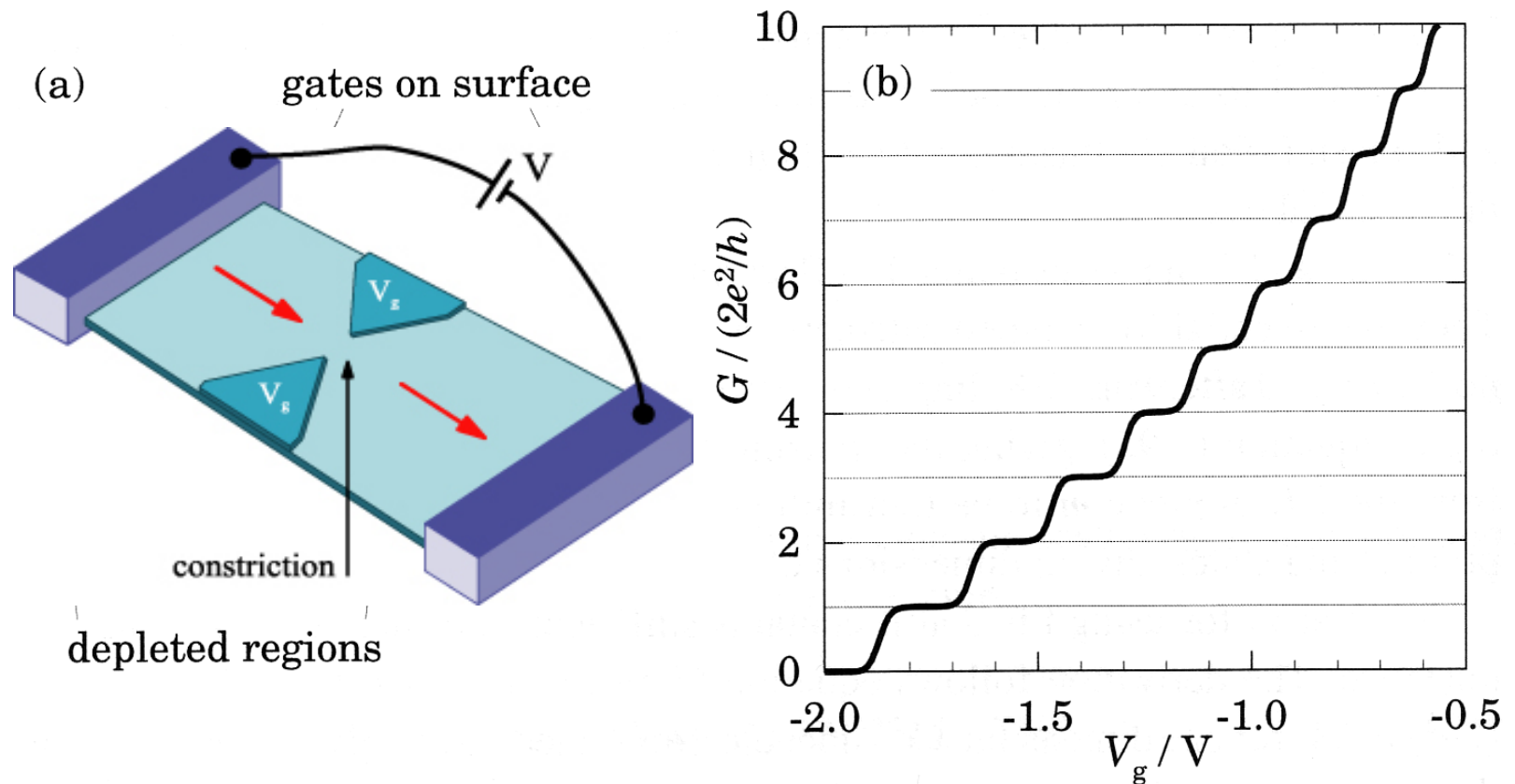


**FIGURE 5.22.** (a) Layout of a typical quantum point contact, a short constriction defined by patterned metal gates on the surface of a heterostructure containing a 2DEG. (b) Calculated conductance  $G(V_g)$  as a function of gate voltage  $V_g$ . [From Nixon, Davies, and Baranger (1991).]

# Quantum point contact

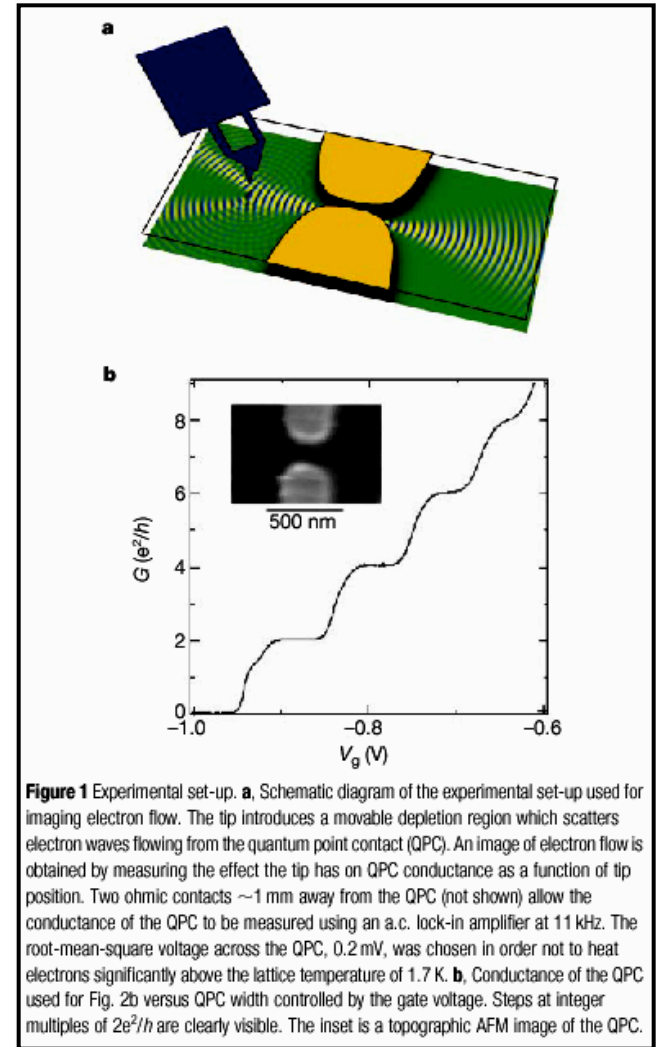
GaAs/AlGaAs interface :  
two-dimensional electron gas

Quantum conductance

$$G = G_0 n$$

$$G_0 = \frac{2e^2}{h} = 7.75 \times 10^{-5} \Omega^{-1}$$

$$n = 1, 2, 3 \dots$$



# Electron flow close to a quantum point contact

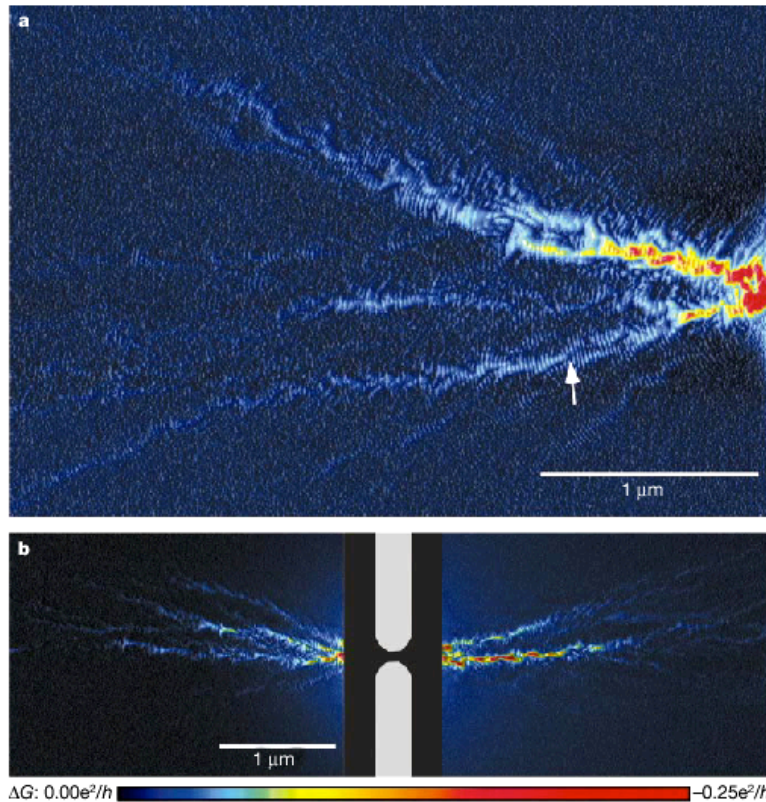


**Figure 2** Experimental images of electron flow. **a**, Image of electron flow from one side of a QPC at  $T = 1.7 \text{ K}$ , biased on the  $G = 2e^2/h$  conductance step. Dark regions correspond to areas where the tip had little effect on QPC conductance, and hence are areas of low electron flow. The colour varies and the height in the scan increases with increasing electron flow. Narrow branching channels of electron flow are visible, and fringes spaced

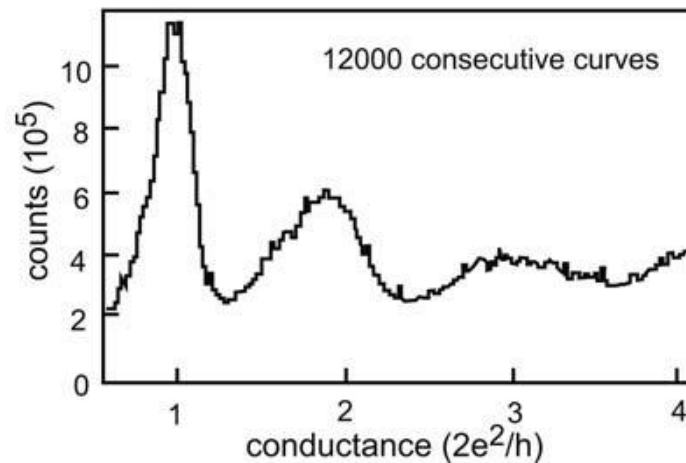
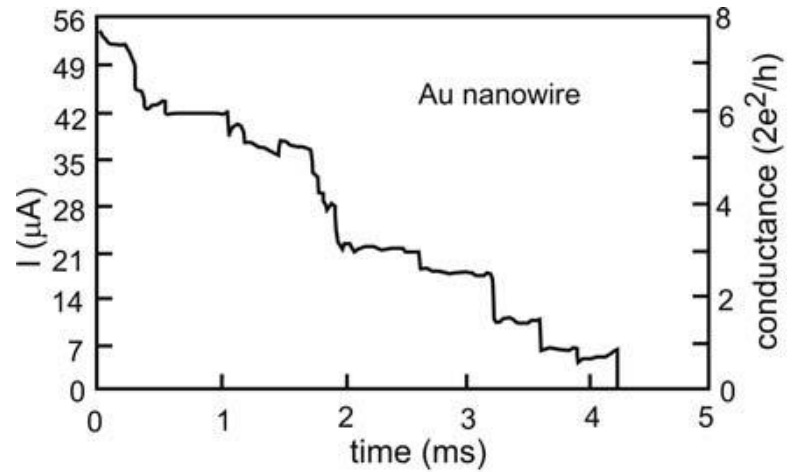
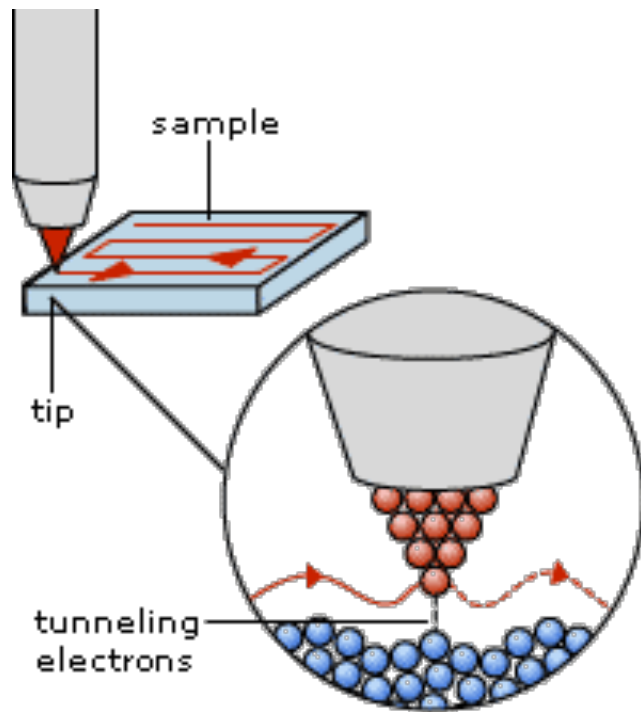
by  $\lambda_F/2$ , half the Fermi wavelength, are seen to persist across the entire scan. **b**, Images of electron flow from both sides of a different QPC, again biased on the  $G = 2e^2/h$  conductance step. The gated region in the centre was not scanned. Strong channelling and branching are again clearly visible. The white arrow points out one example of the formation of a cusp downstream from a dip in the potential.

- Electrons are wave with wave vector  $k_F$
- Interference stripe with

$$\lambda = \frac{1}{2k_F}$$



# Quantum point contact formed in STM





# Molecular Break Junctions

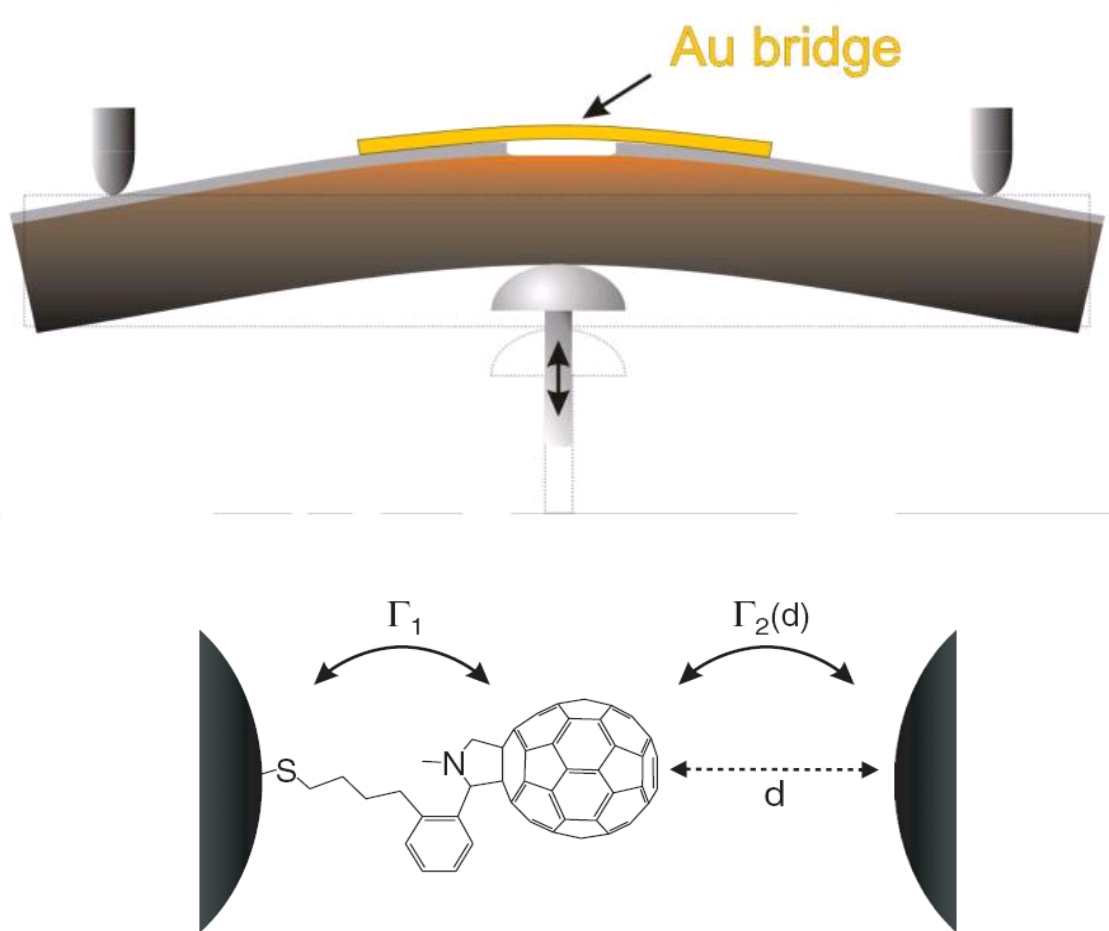


**Figure 1.** Schematic representation of a break junction with a thiolated  $C_{60}$  molecule anchored to the left electrode. The distance  $d$  between the molecule and the right electrode can be adjusted by opening and closing the junction.

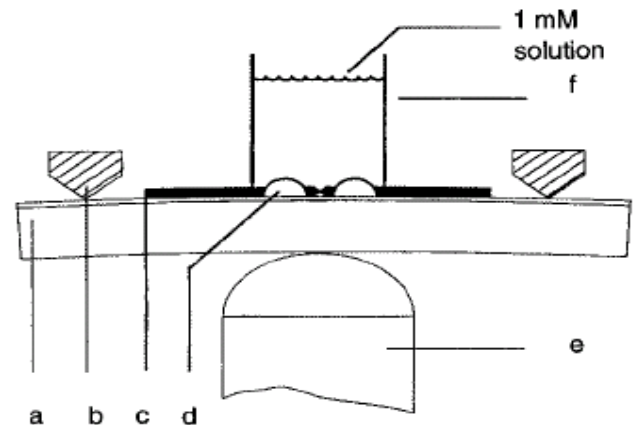
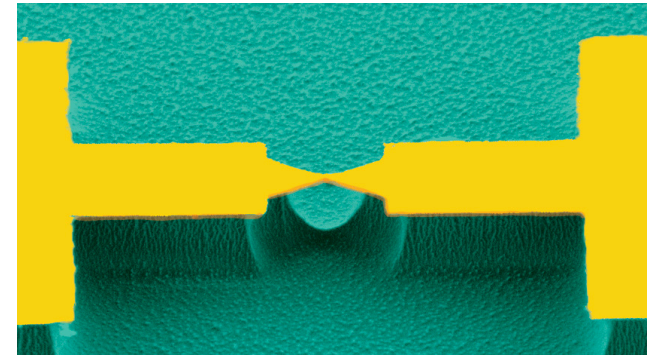


**Fig. 1.** A schematic of the MCB junction with (a) the bending beam, (b) the counter supports, (c) the notched gold wire, (d) the glue contacts, (e) the piezo element, and (f) the glass tube containing the solution.

# Electronic Structure of 0-D Systems

Quantum dots: Quantized energy levels.

$e$  in spherical potential well:  $\varepsilon_{n,l,m} = \varepsilon_{n,l}$   $\psi_{n,l,m}(r, \theta, \phi) = R_{n,l}(r) Y_{l,m}(\theta, \phi)$

For an infinite well with  $V = 0$  for  $r < R$  :

$$\varepsilon_{n,l} = \frac{\hbar^2 \beta_{n,l}^2}{2m^* R^2} \quad R_{n,l}(r) = j_l \left( \frac{\beta_{n,l} r}{R} \right) \quad \text{for } r < R$$

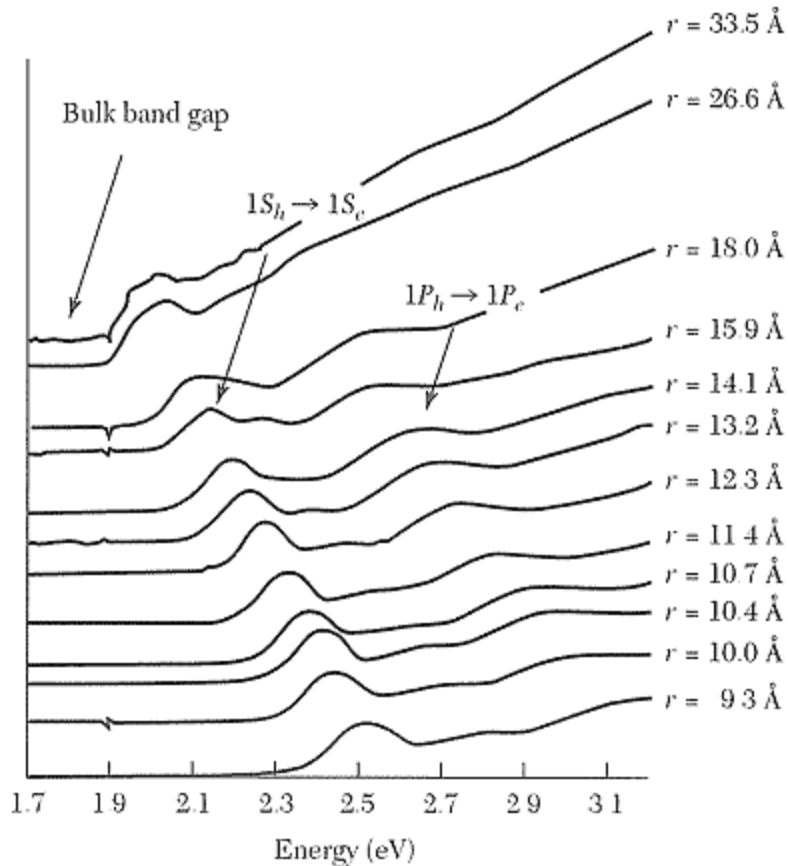
$$\beta_{n,l} = n^{\text{th}} \text{ root of } j_l(x). \quad j_l(\beta_{n,l}) = 0$$

$$\beta_{0,0} = \pi \text{ (1S)}, \quad \beta_{0,1} = 4.5 \text{ (1P)}, \quad \beta_{0,2} = 5.8 \text{ (1D)}$$

$$\beta_{1,0} = 2\pi \text{ (2S)}, \quad \beta_{1,1} = 7.7 \text{ (2P)}$$

# Semiconductor Nanocrystals

## CdSe nanocrystals



For CdSe:

$$m_c^* = 0.13 m \quad \epsilon_{n,l} = \left( \frac{\beta_{n,l}}{\beta_{0,0}} \right)^2 \left( \frac{2.9 \text{ eV}}{R^2} \right)$$

$$\text{For } R = 2 \text{ nm, } \epsilon_{0,1} - \epsilon_{0,0} = 0.76 \text{ eV}$$

For  $e$ ,  $\epsilon_{0,0}$  increases as  $R$  decreases.

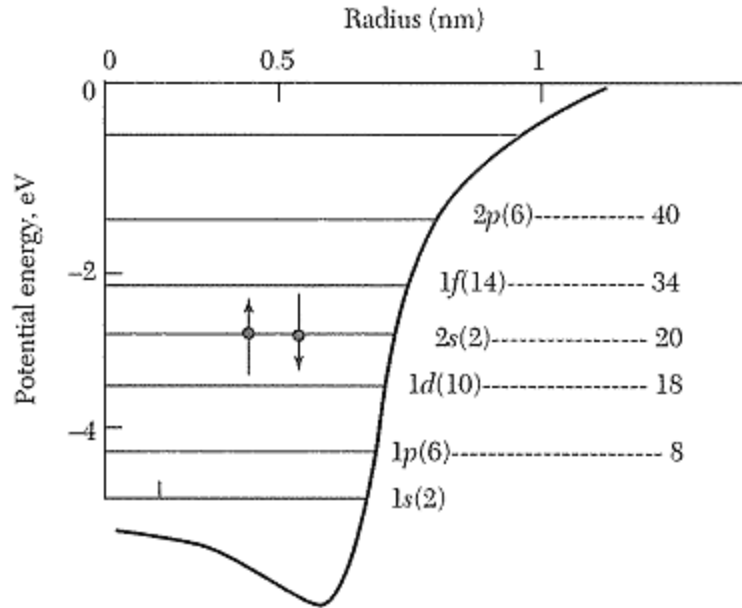
For  $h$ ,  $\epsilon_{0,0}$  decreases as  $R$  decreases.

$\rightarrow E_g$  increases as  $R$  decreases.

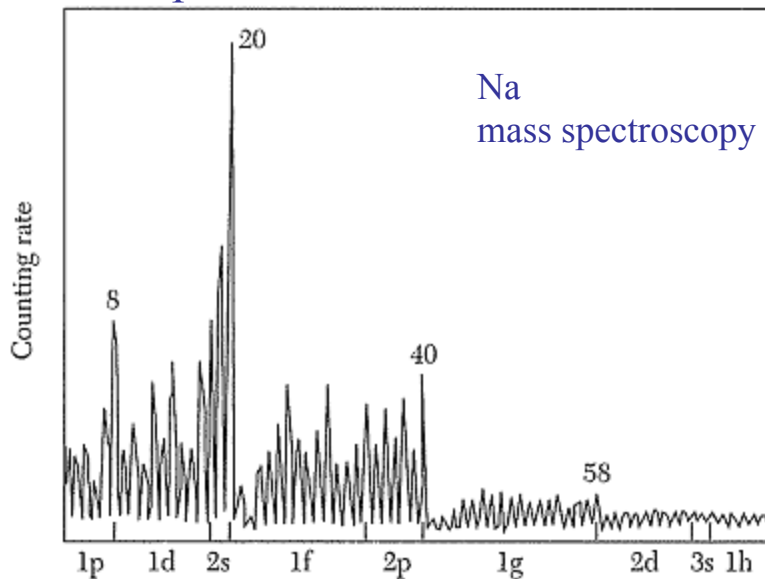
Optical spectra of nanocrystals can be tuned continuously in visible region.

Applications: fluorescent labeling, LED.

# Metallic Dots



Small spherical alkali metallic cluster



Mass spectroscopy (abundance spectra):  
 Large abundance at cluster size of magic numbers ( 8, 20, 40, 58, ... )  
 → enhanced stability for filled  $e$ -shells.

Average level spacing at  $\varepsilon_F$ :

$$\Delta\varepsilon \approx \frac{1}{D(\varepsilon_F)} = \frac{2\varepsilon_F}{3N}$$

For Au nanoparticles with  $R = 2$  nm,  
 $\Delta\varepsilon \approx 2$  meV.

whereas CdSe gives  $\Delta\varepsilon \approx 0.76$  eV.

→  $\varepsilon$  quantization more influential in semiconductor.

Optical properties of metallic dots dominated by surface plasmon resonance.

If retardation effects are negligible,

$$P = \frac{\chi}{1 + \frac{4\pi}{3}\chi} E_{ext}$$

$$\chi(\omega) = -\frac{n e^2}{m \omega^2} \quad \rightarrow \quad P = \frac{1}{\frac{m \omega^2}{n e^2} - \frac{4\pi}{3}} E_{ext} = \frac{3}{4\pi \left( \frac{3 \omega^2}{\omega_p^2} - 1 \right)} E_{ext}$$

Surface plasma mode at singularity:

$$\omega_{sp} = \frac{\omega_p}{\sqrt{3}} \quad \text{indep of } R.$$

For Au or Ag,  $\omega_p \sim \text{UV}$ ,  $\omega_{sp} \sim \text{Visible}$ .

→ liquid / glass containing metallic nanoparticles are brilliantly colored.

Large **E** just outside nanoparticles near resonance enhances weak optical processes.

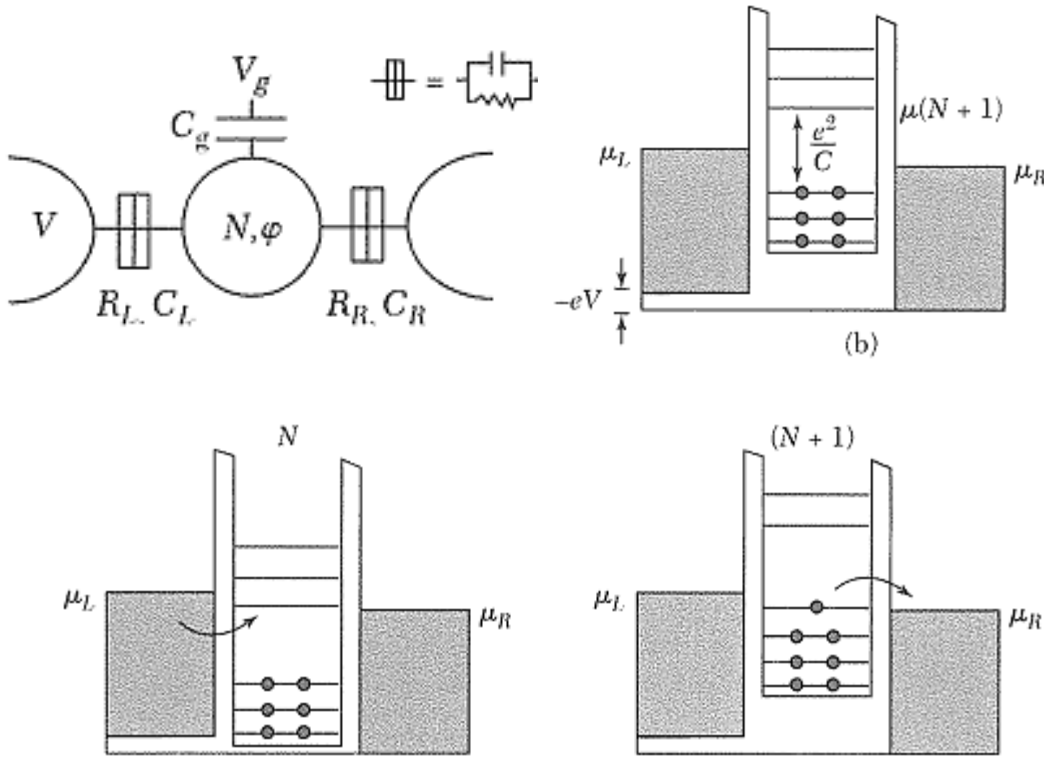
This is made use of in Surface Enhanced Raman Scattering (SERS), & Second Harmonic Generation (SHG).

# Discrete Charge States

Thomas-Fermi approximation:  $\mu_{N+1} = \varepsilon_{N+1} - e\varphi = \varepsilon_{N+1} + NU - \alpha e V_g$

$U$  = interaction between 2  $e$ 's on the dot = **charging energy**.

$\alpha$  = rate at which a nearby gate voltage  $V_g$  shifts  $\varphi$  of the dot.



Neglecting its dependence on state,

$$U = \frac{e^2}{C} \quad \alpha = \frac{C_g}{C}$$

$C$  = capacitance of dot.

$C_g$  = capacitance between gate & dot

If dot is in weak contact with reservoir,  $e$ 's will tunnel into it until the  $\mu$ 's are equalized.

Change in  $V_g$  required to add an  $e$  is

$$\Delta V_g = \frac{1}{\alpha e} \left( \varepsilon_{N+1} - \varepsilon_N + \frac{e^2}{C} \right)$$

$U$  depends on size & shape of dot & its local environment.

For a spherical dot of radius  $R$  surrounded by a spherical metal shell of radius  $R + d$ ,

$$U = \frac{e^2}{\epsilon} \frac{d}{R(R+d)}$$

For  $R = 2$  nm,  $d = 1$  nm &  $\epsilon = 1$ , we have

$$U = 0.24 \text{ eV} \gg k_B T = 0.026 \text{ eV} \quad \text{at } T = 300 \text{ K}$$

→ Thermal fluctuation strongly suppressed.

For metallic dots of 2 nm radius,  $\Delta\epsilon \approx 2 \text{ meV} \rightarrow \Delta V_g$  due mostly to  $U$ .

For semiC dots, e.g., CdSe,  $\Delta\epsilon \approx 0.76 \text{ eV} \rightarrow \Delta V_g$  due both to  $\Delta\epsilon$  &  $U$ .

Charging effect is destroyed if tunneling rate is too great.

Charge resides in dot for time  $\delta t \approx RC$ . ( $R$  = resistance)

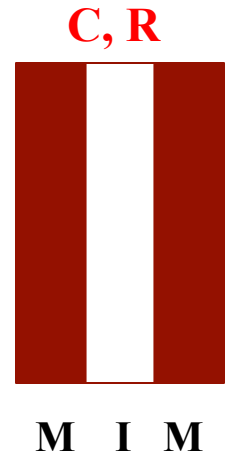
$$\rightarrow \quad \delta\epsilon \approx \frac{h}{\delta t} \approx \frac{h}{RC} = \frac{e^2}{C} \frac{h}{e^2} \frac{1}{R}$$

Quantum fluctuation smears out charging effect when  $\delta\epsilon \approx U$ , i.e., when  $R \sim h / e^2$ .

# Conditions for a Coulomb Blockade

1) The Coulomb energy  $e^2/C$  needs to exceed the thermal energy  $k_B T$ .

Otherwise an extra electron can get onto the dot with thermal energy instead of being blocked by the Coulomb energy. A dot needs to be either small ( $< 10$  nm at 300K) or cold ( $< 1$  K for a  $\mu\text{m}$  sized dot).



2) The residence time  $\Delta t = RC$  of an electron on the dot needs to be so long that the corresponding energy uncertainty  $\Delta E = h/\Delta t = h/RC$  is less than the Coulomb energy  $e^2/C$ . That leads to a condition for the tunnel resistance between the dot and source/drain:  $R > h/e^2$   
 $\approx 26 \text{ k}\Omega$



$$\langle R + dR \rangle = \langle R \rangle \left( 1 + 2 \frac{dL}{l_e} \right) \rightarrow \langle dR \rangle = \langle R \rangle \frac{2dL}{l_e}$$

$$\therefore \ln \frac{\langle R \rangle}{\langle R \rangle_0} = \frac{2L}{l_e} \quad \text{where} \quad \langle R \rangle_0 = \langle R \rangle|_{L=0} = R_Q = \frac{h}{2e^2}$$

$$\langle R \rangle = \frac{h}{2e^2} \exp\left(\frac{2L}{l_e}\right) \quad \text{C.f. Ohm's law } R \propto L$$

For a 1-D system with disorder, all states become localized to some length  $\xi$ .

Absence of extended states  $\rightarrow R \propto \exp(a L / \xi)$ ,  $a$  = some constant.

For quasi-1-D systems, one finds  $\xi \sim N l_e$ , where  $N$  = number of occupied subbands.

For  $T > 0$ , interactions with phonons or other  $e$ 's reduce phase coherence to length  $l_\varphi = A T^{-\alpha}$ .

$$\therefore \langle R \rangle \approx \frac{h}{2e^2} \exp\left(\frac{2l_\varphi}{l_e}\right) \quad \text{for each coherent segment.}$$

Overall  $\langle R \rangle \approx$  incoherent addition of  $L / l_\varphi$  such segments.

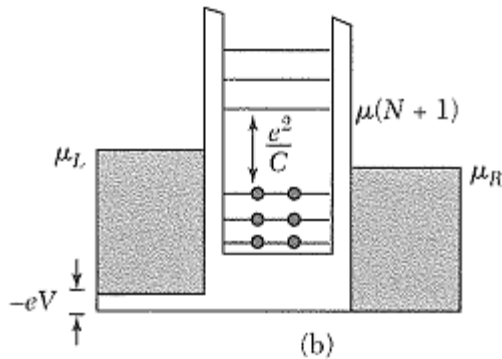
For sufficiently high  $T$ ,  $l_\varphi \leq l_e$ , coherence is effectively destroyed & ohmic law is recovered.

All states in disordered 2-D systems are also localized.

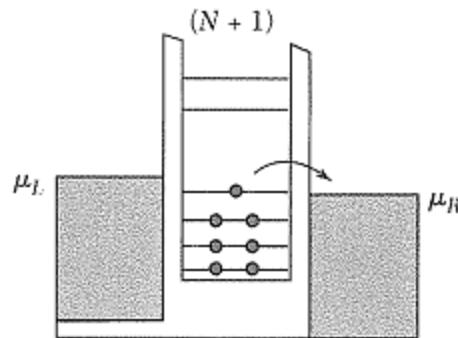
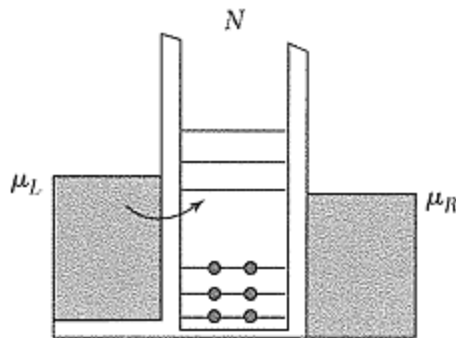
Only some states (near band edges) in disordered 3-D systems are localized.

# Electrical Transport in 0-D

For  $T < (U + \Delta\varepsilon) / k_B$ ,  $U$  &  $\Delta\varepsilon$  control  $e$  flow thru dot.



Transport thru dot is suppressed when  $\mu_L$  &  $\mu_R$  of leads lie between  $\mu_N$  &  $\mu_{N+1}$  (**Coulomb blockade**)



Transport is possible only when  $\mu_{N+1}$  lies between  $\mu_L$  &  $\mu_R$ .

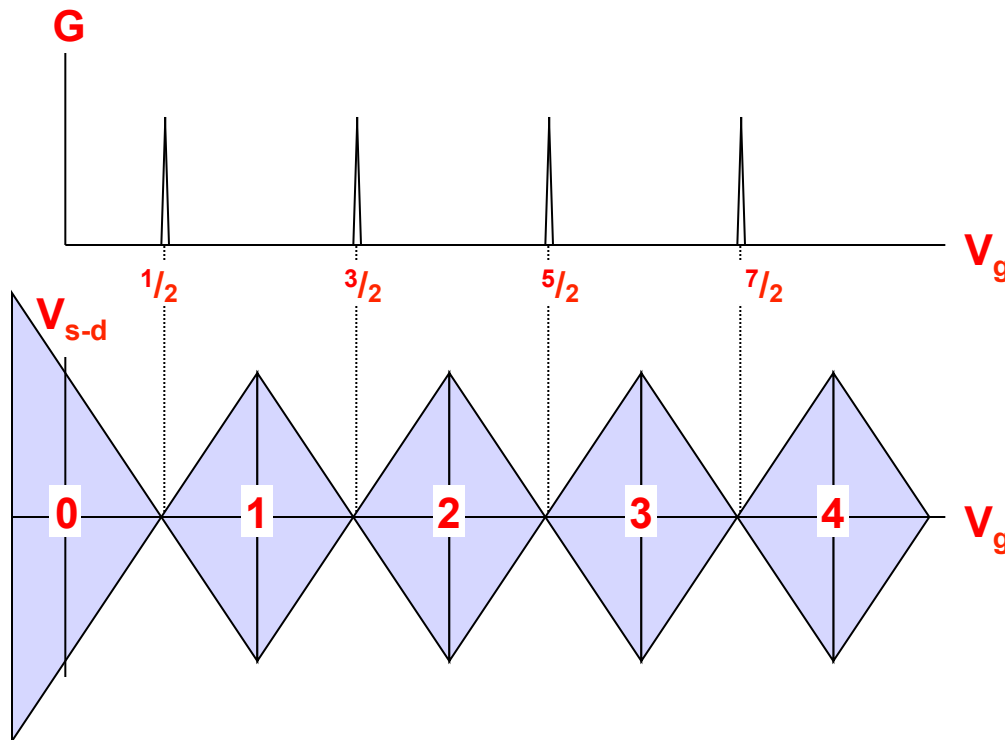
→ Coulomb oscillations of  $G(V_g)$ .

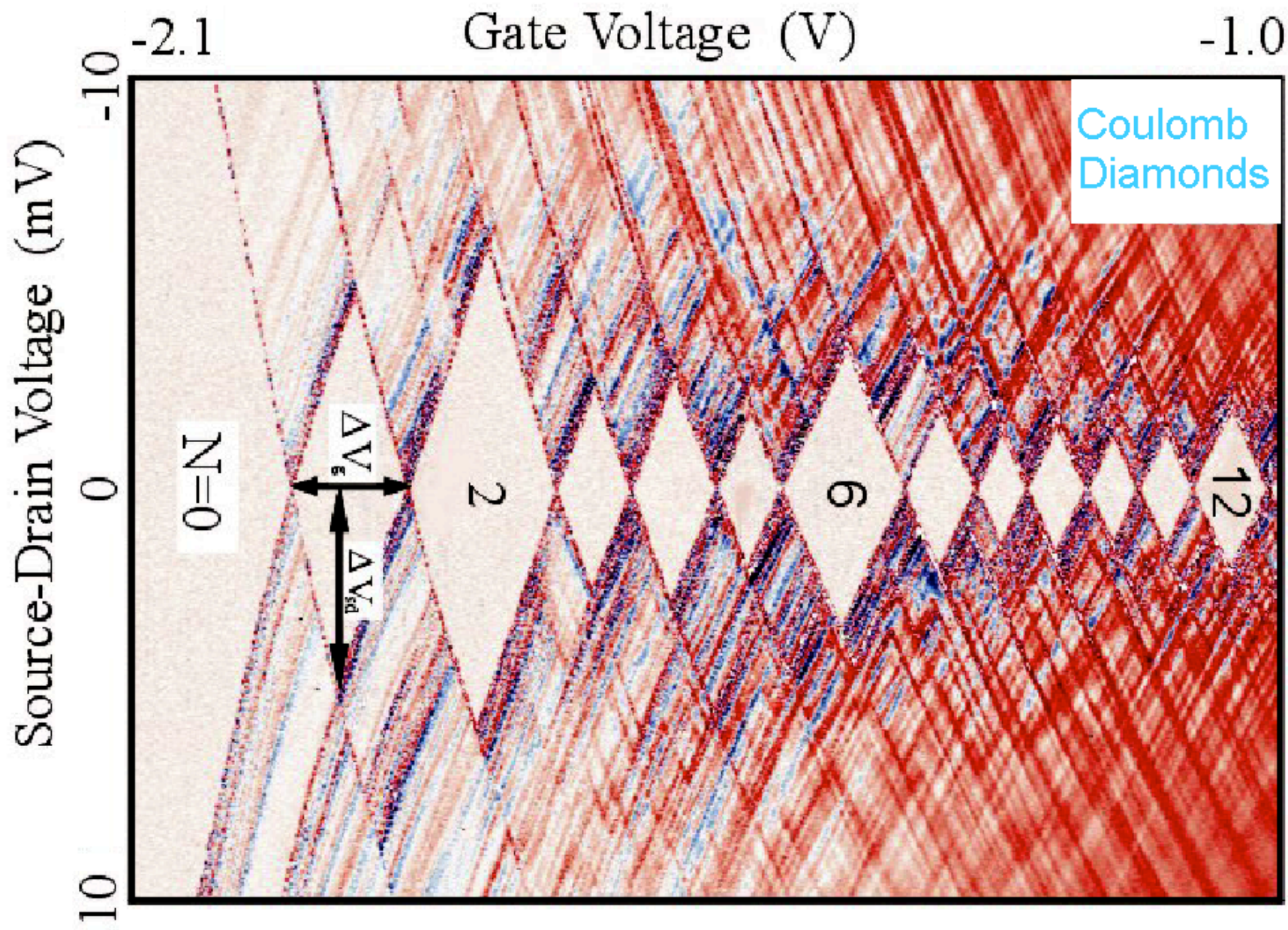
# Gate Voltage versus Source-Drain Voltage

The situation gets a bit confusing, because there are two voltages that can be varied, the gate voltage  $V_g$  and the source-drain voltage  $V_{s-d}$ .

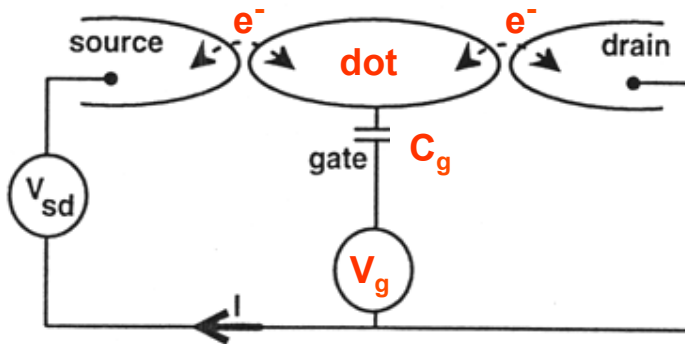
Both affect the conductance. Therefore, one often plots the conductance  $G$  against both voltages (see the next slide for data).

Schematically, one obtains “Coulomb diamonds”, which are regions with a stable electron number  $N$  on the dot (and consequently zero conductance).





# Single Electron Transistor (SET)



A single electron transistor is similar to a normal transistor (below), except

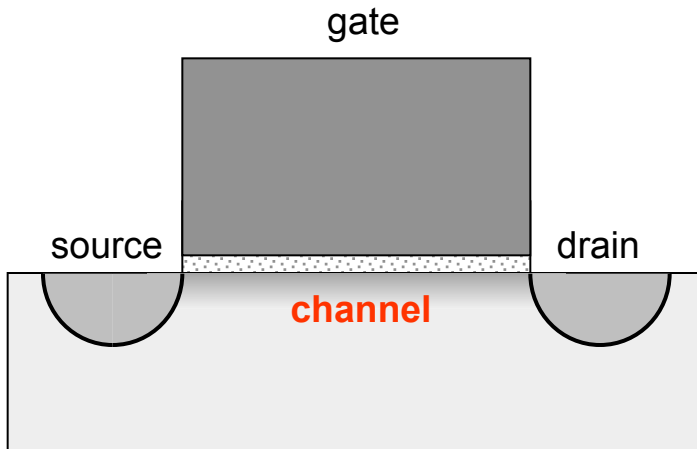
- 1) the channel is replaced by a small dot.
- 2) the dot is separated from source and drain by thin insulators.

An electron tunnels in two steps:

source  $\rightarrow$  dot  $\rightarrow$  drain

The gate voltage  $V_g$  is used to control the charge on the gate-dot capacitor  $C_g$ .

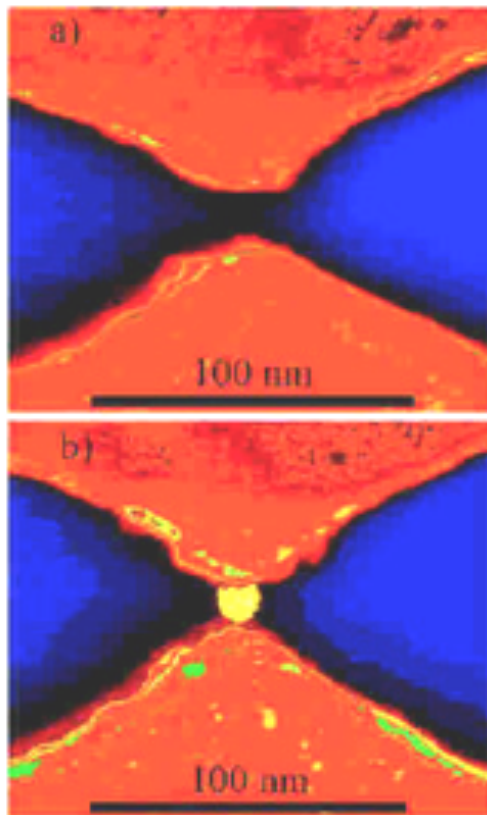
How can the charge be controlled with the precision of a single electron?



Kouwenhoven et al., *Few Electron Quantum Dots*, Rep. Prog. Phys. **64**, 701 (2001).

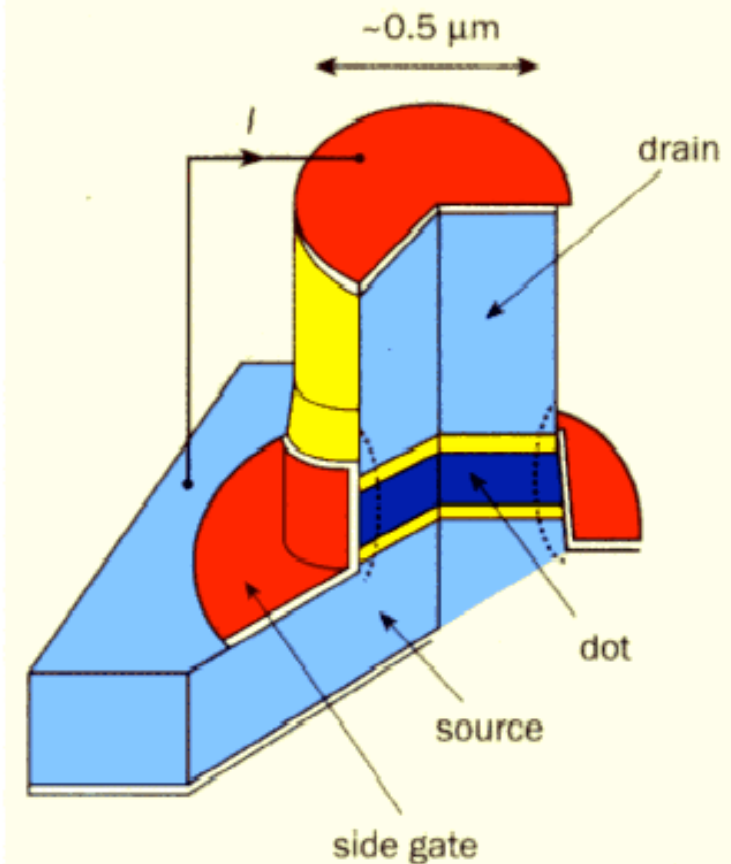


# Designs for Single Electron Transistors



Nanoparticle attracted electrostatically to the gap between source and drain electrodes. The gate is underneath.

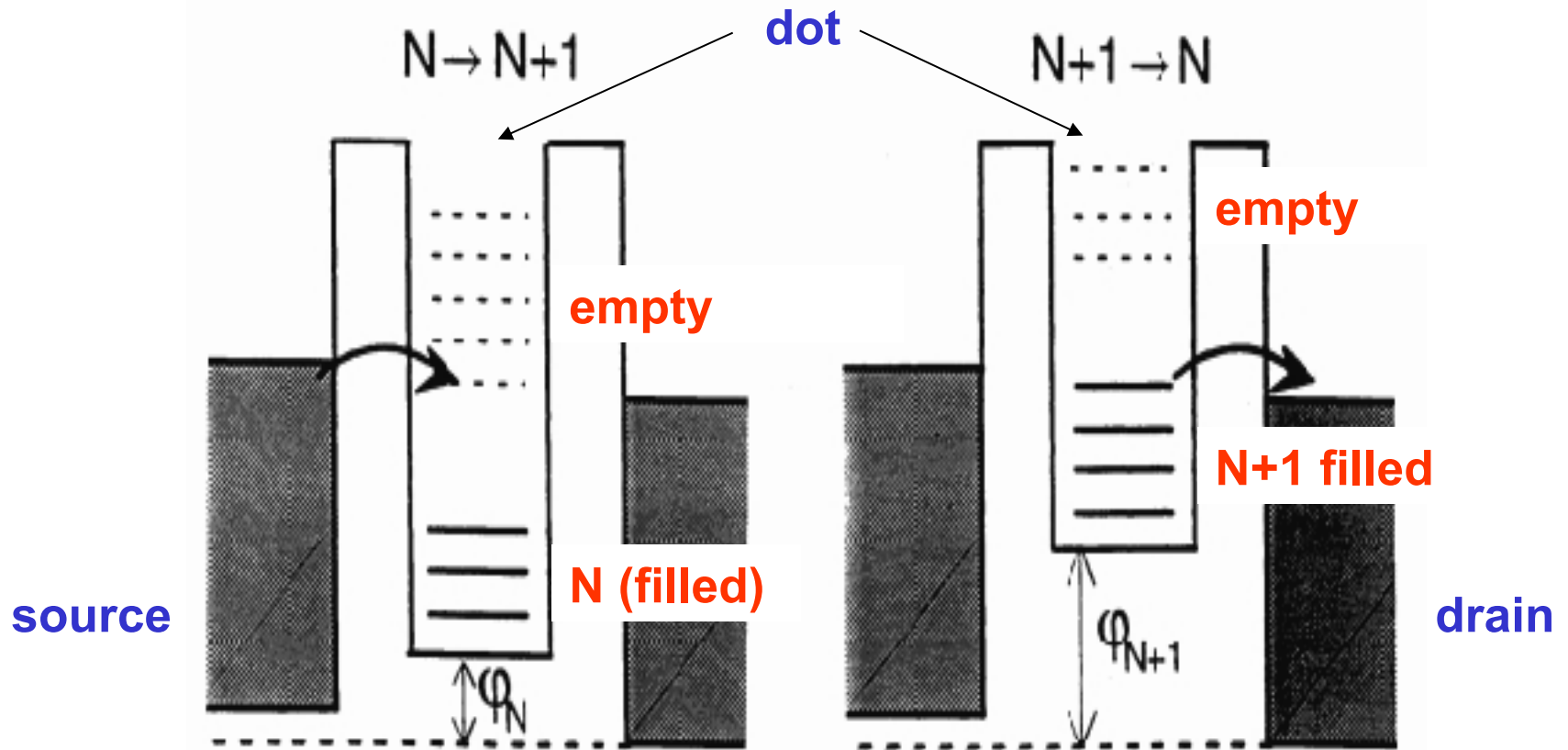
## 1 Vertical quantum dot structure



The quantum-dot structure studied at Delft and NTT in Japan is fabricated in the shape of a round pillar. The source and drain are doped semiconductor layers that conduct electricity, and are separated from the quantum dot by tunnel barriers 10 nm thick. When a negative voltage is applied to the metal side gate around the pillar, it reduces the diameter of the dot from about 500 nm to zero, causing electrons to leave the dot one at a time.

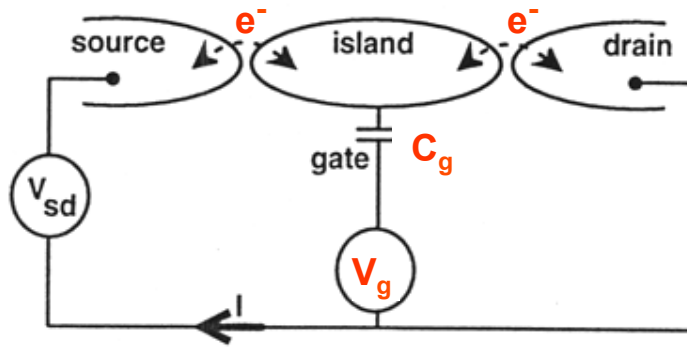
# Two Step Tunneling

source  $\rightarrow$  dot  $\rightarrow$  drain



(For a detailed explanation see the annotation in the .ppt version.)

# Charging a Dot, One Electron at a Time

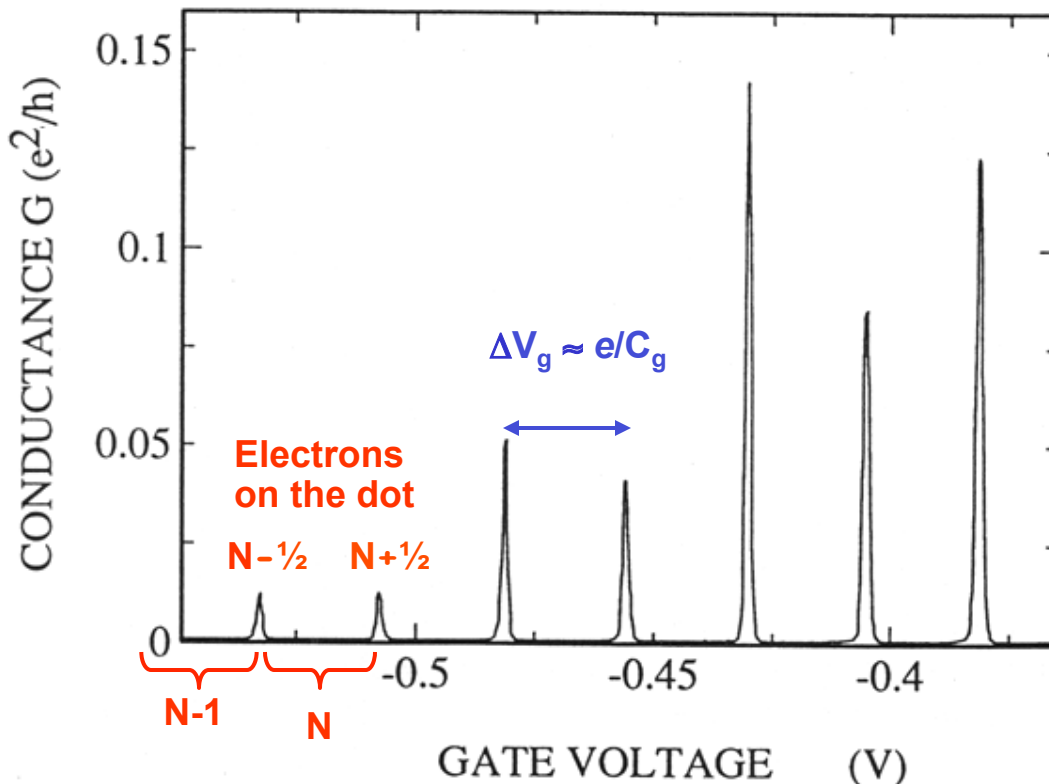


Sweeping the gate voltage  $V_g$  changes the charge  $Q_g$  on the gate-dot capacitor  $C_g$ . To add one electron requires the voltage  $\Delta V_g \approx e/C_g$  since  $C_g = Q_g/V_g$ .

The source-drain conductance  $G$  is zero for most gate voltages, because putting even one extra electron onto the dot would cost too much Coulomb energy. This is called **Coulomb blockade**.

Electrons can hop onto the dot only at a gate voltage where the number of electrons on the dot flip-flops between  $N$  and  $N+1$ . Their time-averaged number is  $N+1/2$  in that case.

The spacing between these half-integer conductance peaks is an integer.



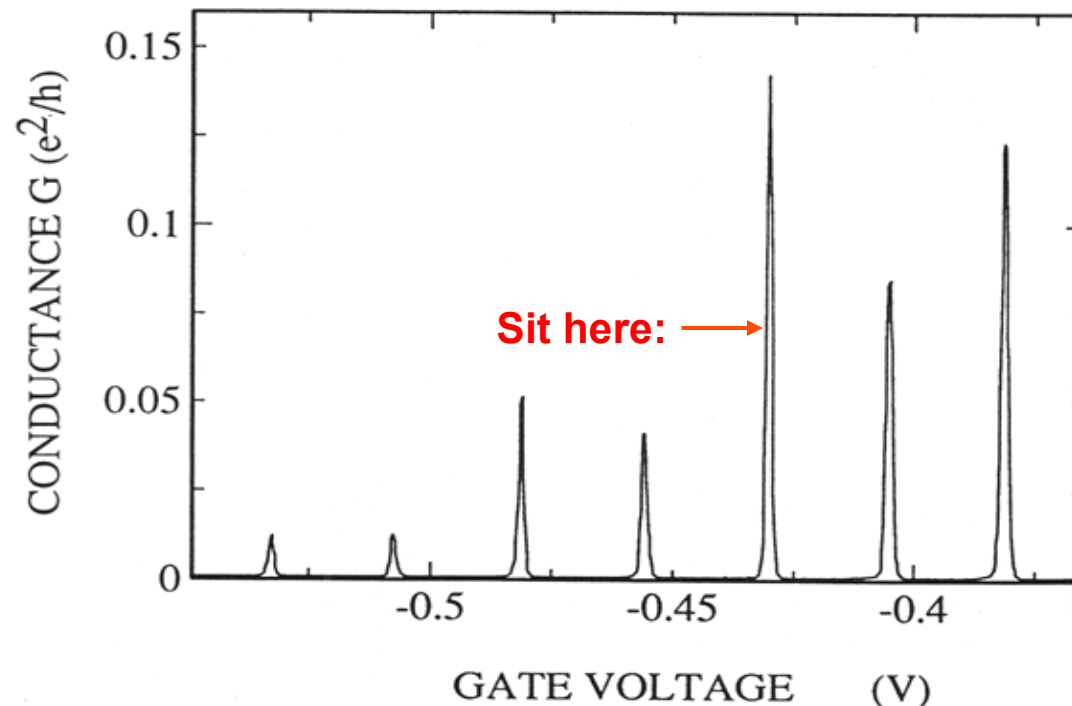


# SET as Extremely Sensitive Charge Detector

At low temperature, the conductance peaks in a SET become very sharp.

Consequently, a very small change in the gate voltage half-way up a peak produces a large current change, i.e. a **large amplification**. That makes the SET extremely sensitive to tiny charges.

The flip side of this sensitivity is that a SET detects every nearby electron. When it hops from one trap to another, the SET produces a noise peak.

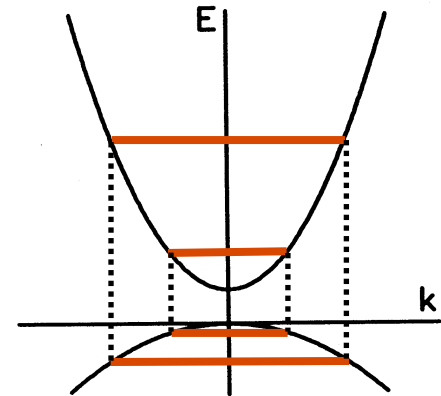


# Including the Energy Levels of a Quantum Dot

Contrary to the Coulomb blockade model, the data show Coulomb diamonds with uneven size. Some electron numbers have particularly large diamonds, indicating that the corresponding electron number is particularly stable.

This is reminiscent of the closed electron shells in atoms. Small dots behave like artificial atoms when their size shrinks down to the electron wavelength.

Continuous energy bands become quantized (see Lecture 8). Adding one electron requires the Coulomb energy  $U$  plus the difference  $\Delta E$  between two quantum levels (next slide). If a second electron is added to the same quantum level (the same shell in an atom),  $\Delta E$  vanishes and only the Coulomb energy  $U$  is needed.



The quantum energy levels can be extracted from the spacing between the conductance peaks by subtracting the Coulomb energy  $U = e^2/C$ .

# Precision Standards from “Single” Electronics

Count individual electrons, pairs, flux quanta

Current I  
Coulomb  
Blockade

$$I = e f$$

Voltage V  
Josephson  
Effect

$$V = h/2e \cdot f$$

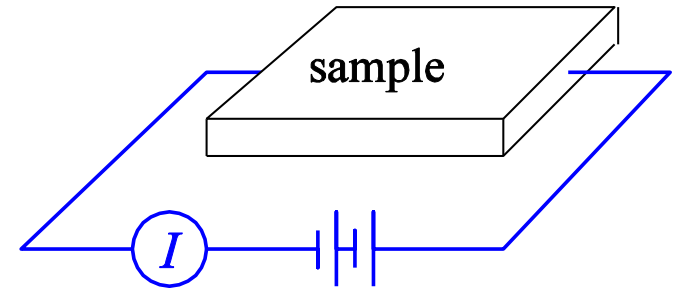
$$V/I = R = h/e^2$$

Resistance R  
Quantum  
Hall Effect

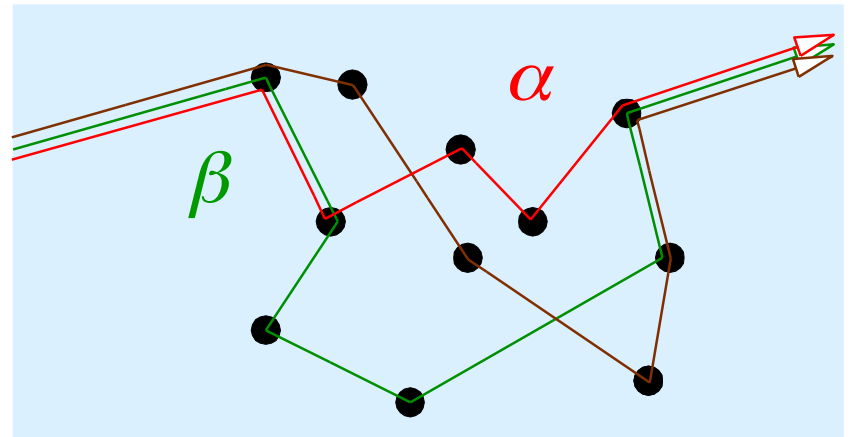
(f = frequency)

# Quantum interference

$$\begin{aligned} g &= \sum_{m,n} |t_{nm}|^2 \\ &= \sum_{m,n} \sum_{\alpha} |t_{nm,\alpha}|^2 + \sum_{m,n} \sum_{\alpha \neq \beta} t_{nm,\alpha} (t_{nm,\beta})^* \\ &= g_{\text{class}} + \delta g \end{aligned}$$



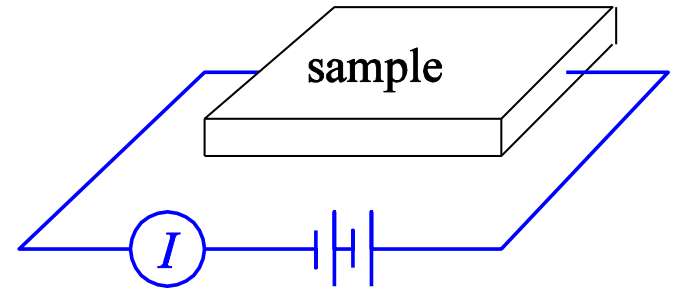
In general:  $\delta g$  small,  
random sign



$t_{nm,\alpha}$ ,  $t_{nm,\beta}$ : amplitude for  
transmission along paths  $\alpha$ ,  $\beta$

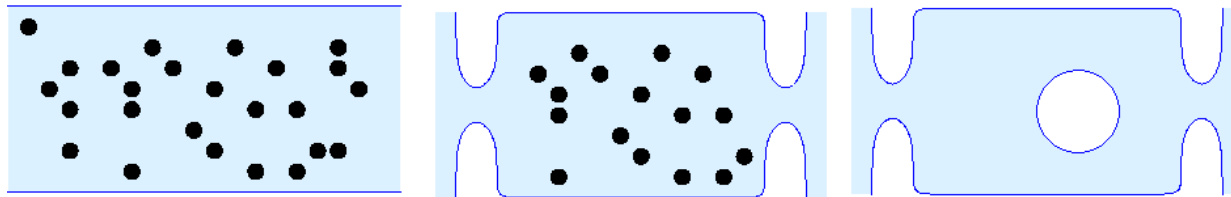
# Quantum interference

$$\begin{aligned} g &= \sum_{m,n} |t_{nm}|^2 \\ &= \sum_{m,n} \sum_{\alpha} |t_{nm,\alpha}|^2 + \sum_{m,n} \sum_{\alpha \neq \beta} t_{nm,\alpha} (t_{nm,\beta})^* \\ &= g_{\text{class}} + \delta g \end{aligned}$$



Three prototypical examples:

- Disordered wire
- Disordered quantum dot
- Ballistic quantum dot



# Scattering matrix and Green function

Recall: retarded Green function is solution of

$$(\varepsilon - \mathcal{H})\mathcal{G}^{\text{R}}(\mathbf{r}, \mathbf{r}'; \omega) = \delta(\mathbf{r} - \mathbf{r}'),$$

In one dimension:

$$\mathcal{G}^{\text{R}}(x, x'; \varepsilon) = -\frac{i}{\hbar v} e^{ik|x-x'|},$$

Green function in channel basis:

$$\varepsilon_k = \varepsilon \text{ and } v = \hbar^{-1} d\varepsilon_k/dk$$

$$\mathcal{G}^{\text{R}}(\mathbf{r}, \mathbf{r}'; \varepsilon) = \sum_{m=1}^{N_j} \sum_{n=1}^{N_k} \mathcal{G}_{m,j;n,k}^{\text{R}}(x, x'; \varepsilon) \chi_{m,j}(y) \chi_{n,k}(y').$$

$\mathbf{r}$  in lead  $j$ ;  $\mathbf{r}'$  in lead  $k$

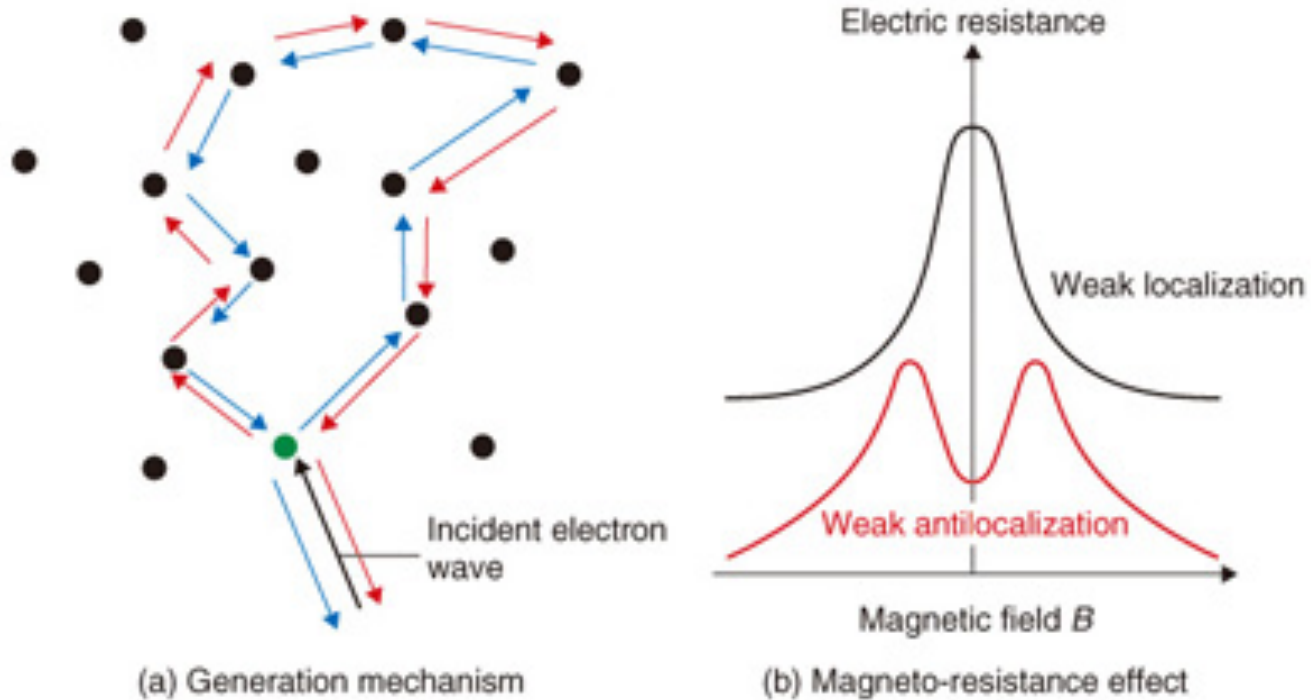
Substitute 1d form of Green function

$$\mathcal{G}_{mn}^{\text{R}}(x, x') = -\frac{i}{\hbar v_m} \delta_{mn} \delta_{jk} e^{ik_m|x-x'|} - \frac{i}{\hbar (v_m v_n)^{1/2}} S_{m,j;n,k} e^{ik_m|x| + ik_n|x'|}.$$

If  $j \neq k$ :  $S_{m,j;n,k} = i\hbar (v_m v_n)^{1/2} \mathcal{G}_{m,k;n,k}^{\text{R}}(0, 0, \varepsilon)$

$$= i\hbar (v_m v_n)^{1/2} \int dy \int dy' \chi_{m,j}(y) \chi_{n,k}(y') \mathcal{G}^{\text{R}}(\mathbf{r}, \mathbf{r}'; \varepsilon)$$

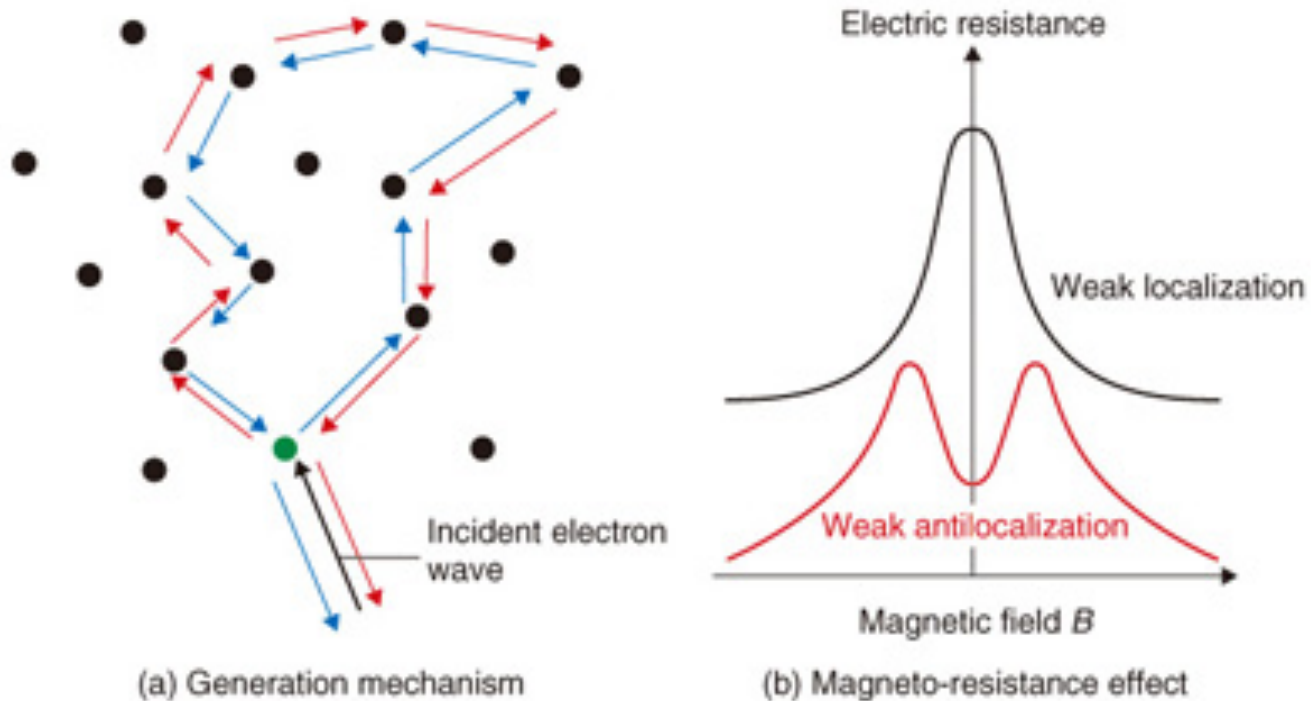
# Weak localization



$$A^2 = (A_1 + A_2)^2 = A_1^2 + A_2^2 + 2 A_1 A_2 = 4 A_1^2$$

Interference effects double the classical contribution and (slightly) suppress the conductance.

# Weak (anti-) localization



In a system with the carrier's spin coupled to its momentum, the spin of the carrier rotates as it goes around a self-intersecting path, and the direction of this rotation is opposite for the two directions about the loop. Because of this, the two paths of any loop interfere *destructively*, which leads to a *lower* net resistivity. This is called *weak antilocalization*.



# Aharonov-Bohm (A-B) Effect

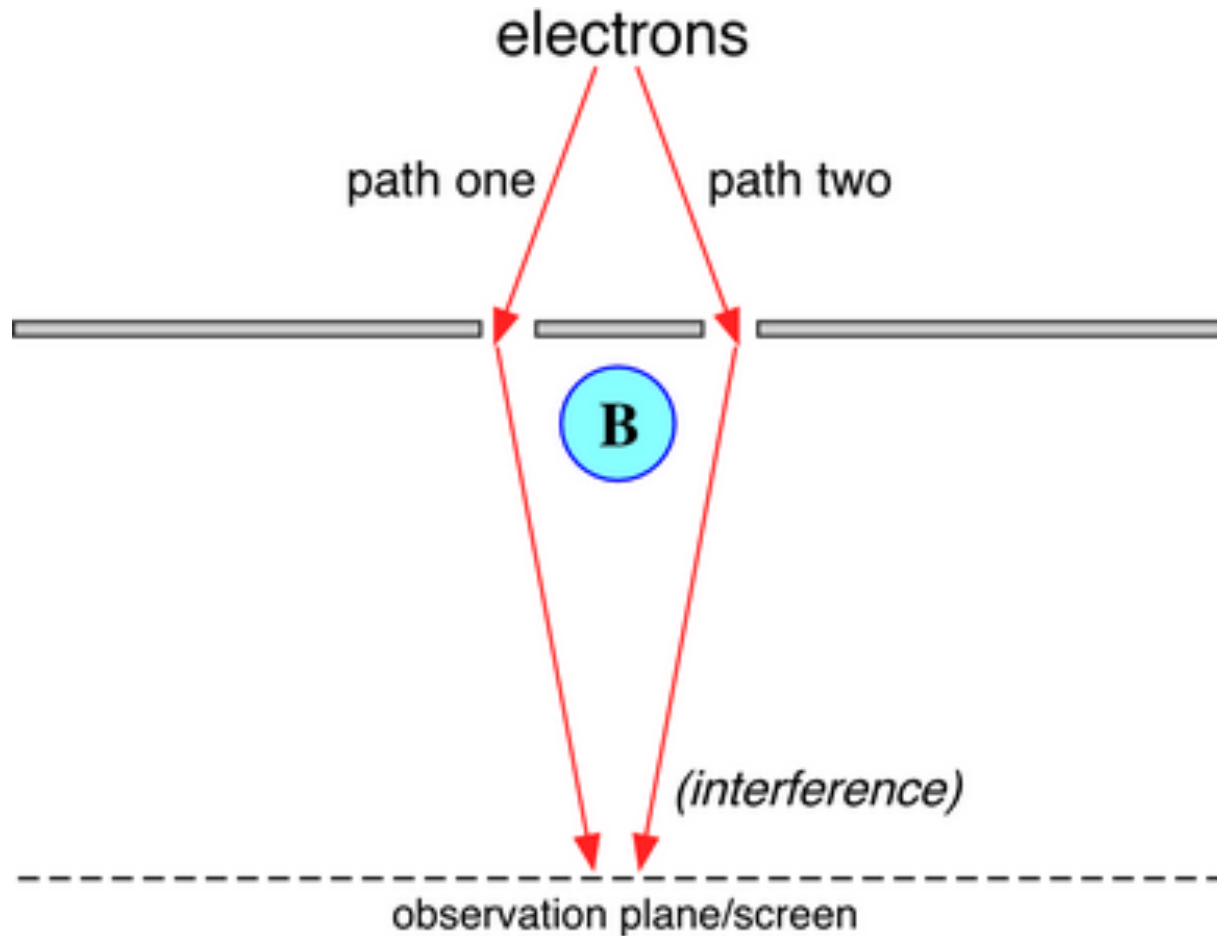


Illustration of interference experiment for Aharonov-Bohm effect

# A-B Effect

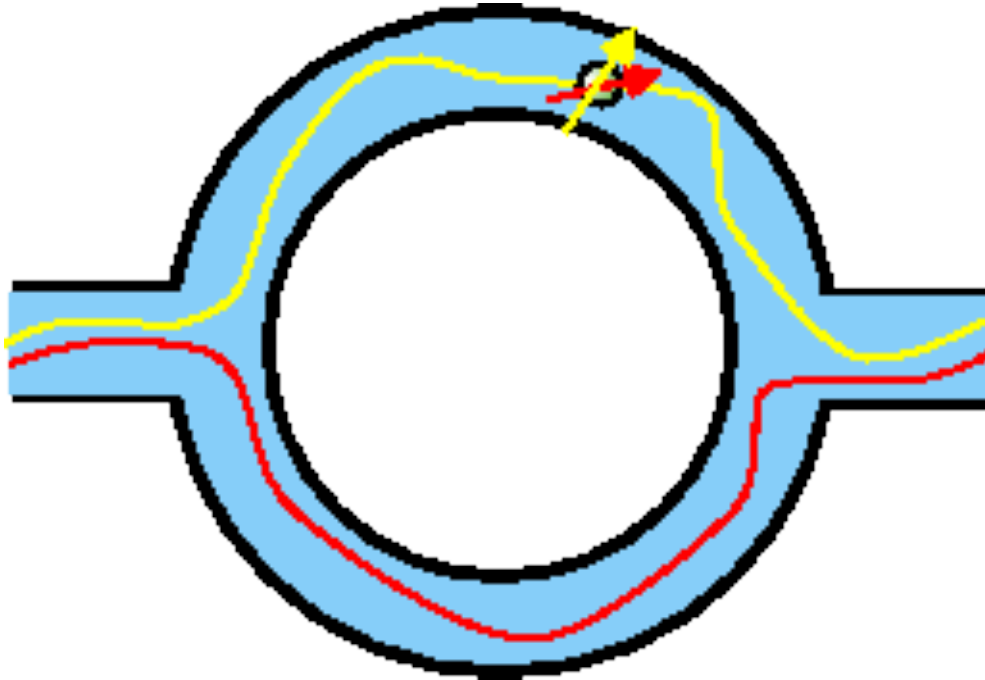
- Formulations

$$\phi = \frac{q}{\hbar} \int_P A \cdot dx$$

$$\Delta\phi = \frac{q\Phi}{\hbar} \quad (\text{Magnetic A-B Effect})$$

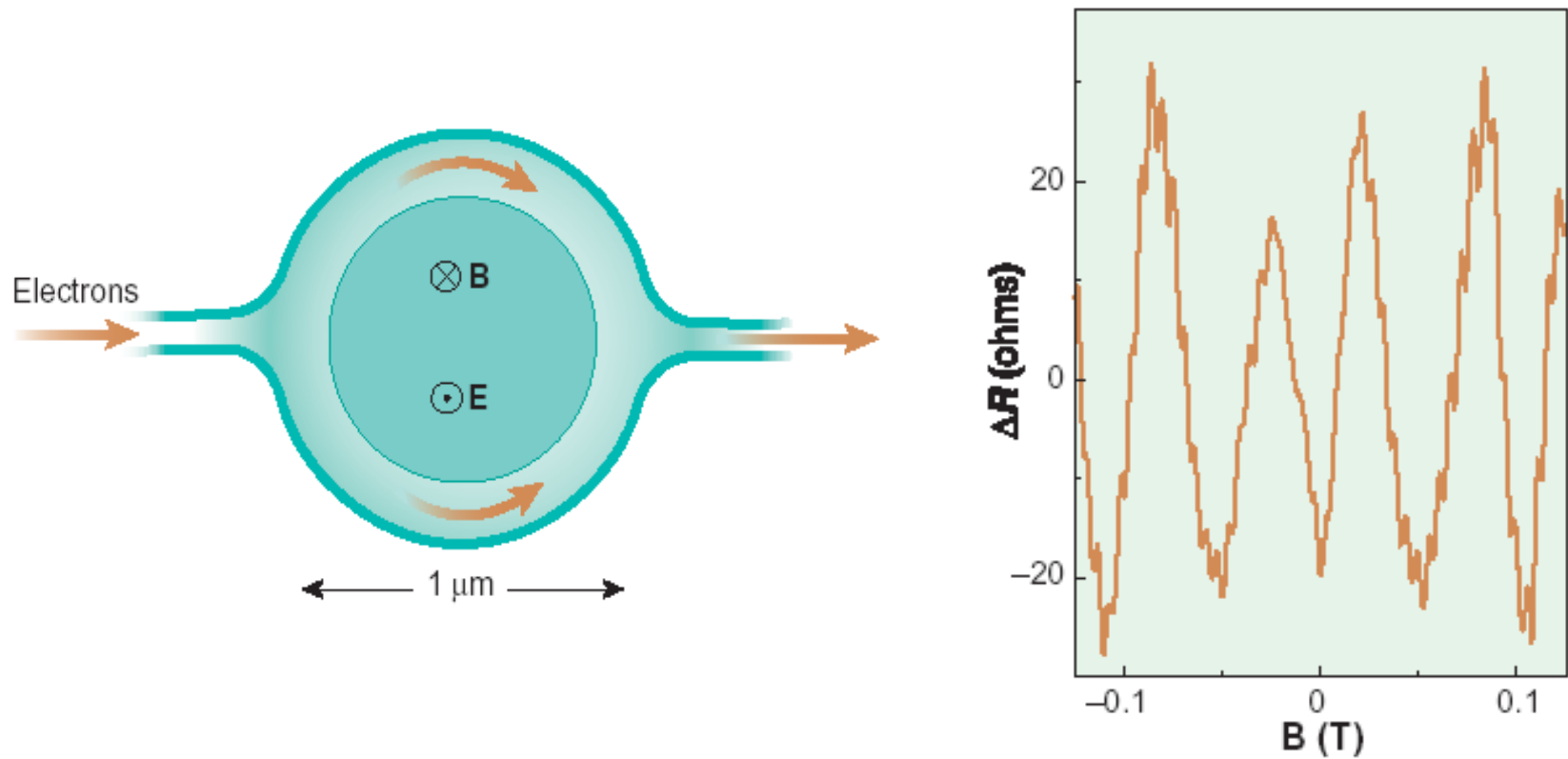
$$\Delta\phi = -\frac{qVt}{\hbar} \quad (\text{Electric A-B Effect})$$

# Ring Oscillations



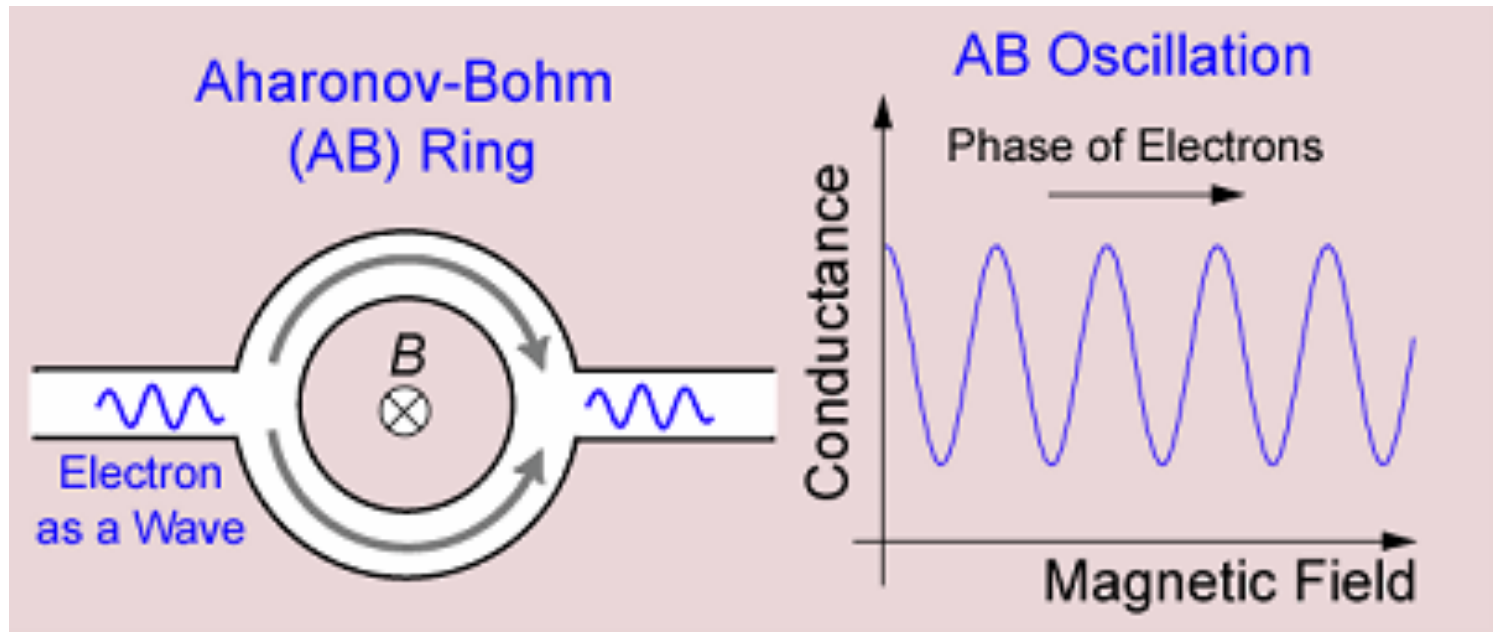
Ring Oscillation without E/B Field

# Ring Oscillations



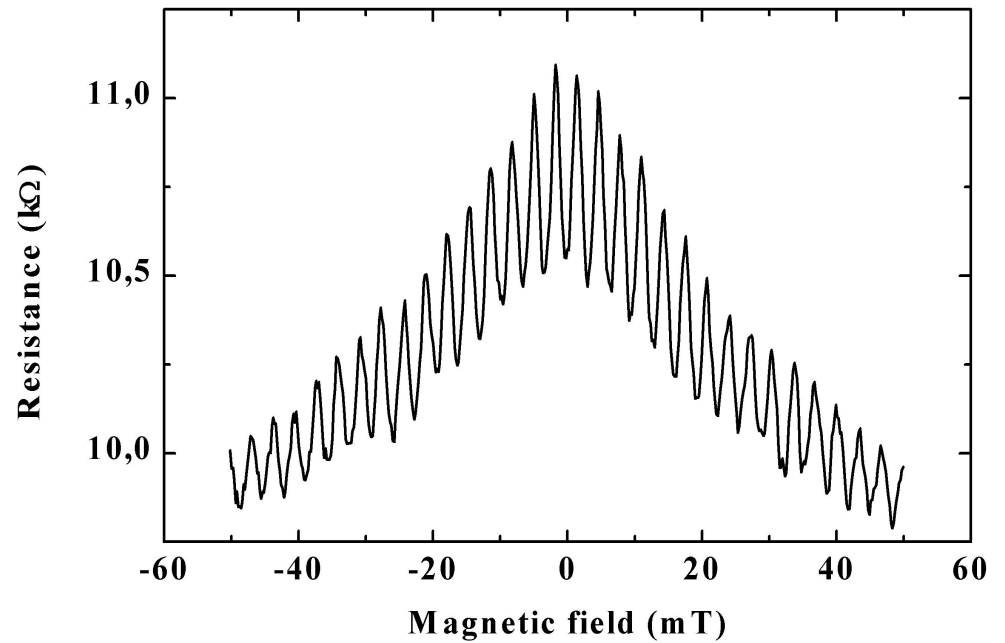
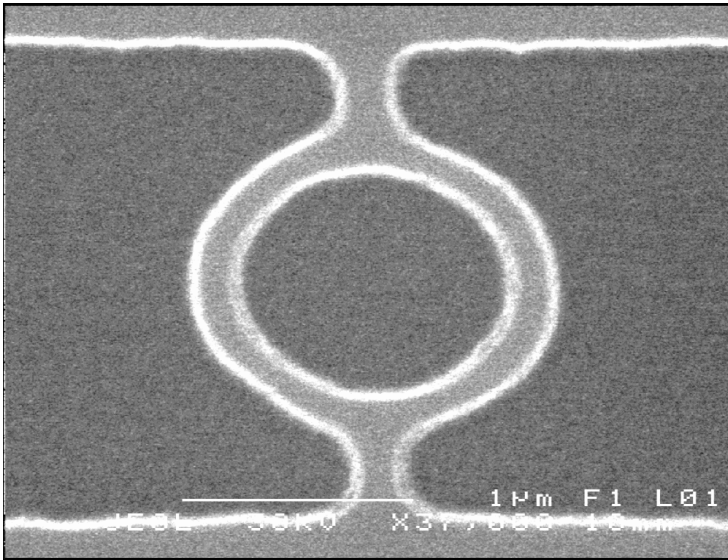
Ring Oscillations with E/B Field

# Ring Oscillation



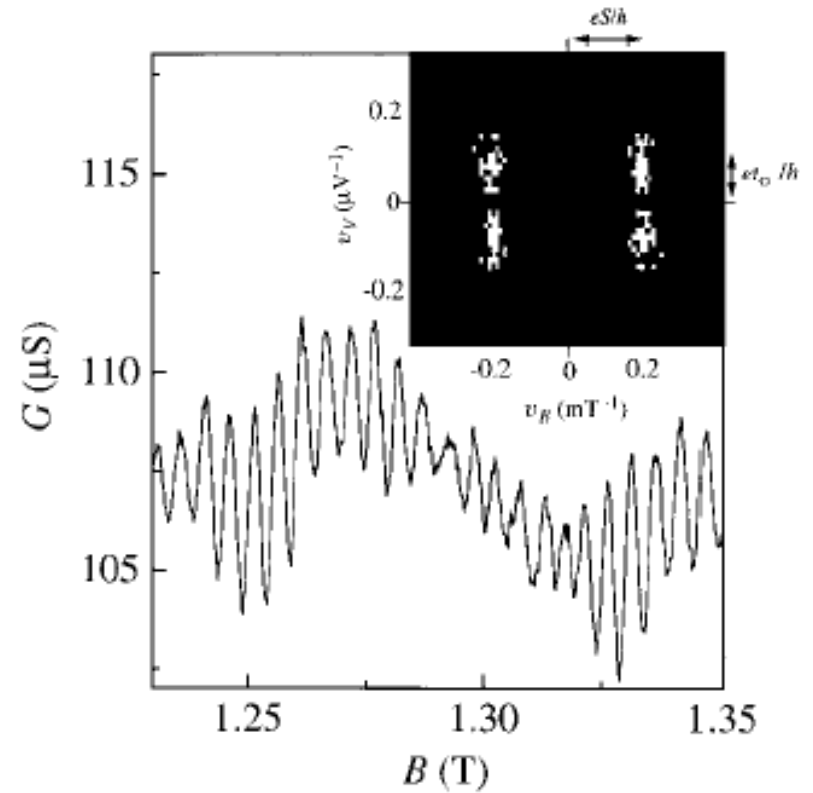
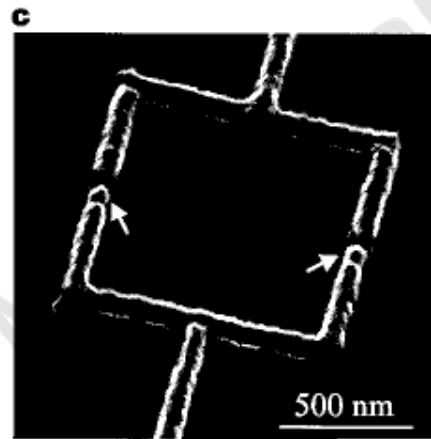
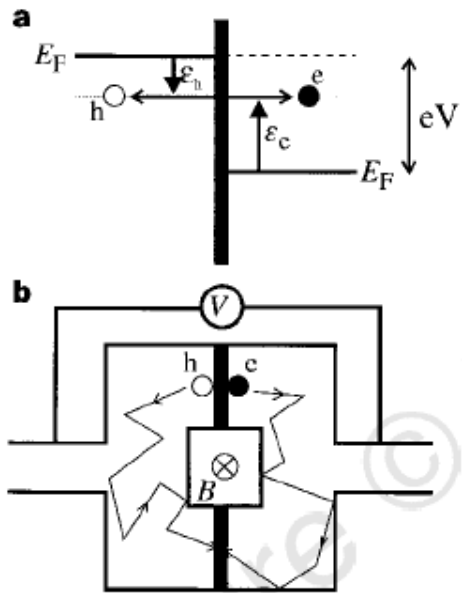
$$\Delta R = \frac{\pi r^2 B}{NWt2e}$$

# A-B Ring Applications



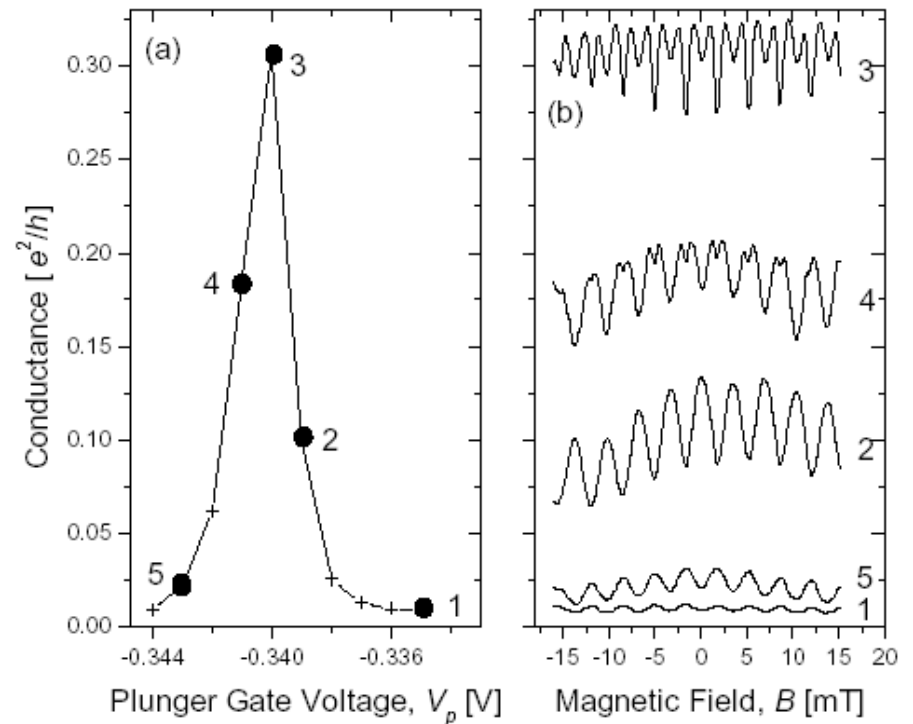
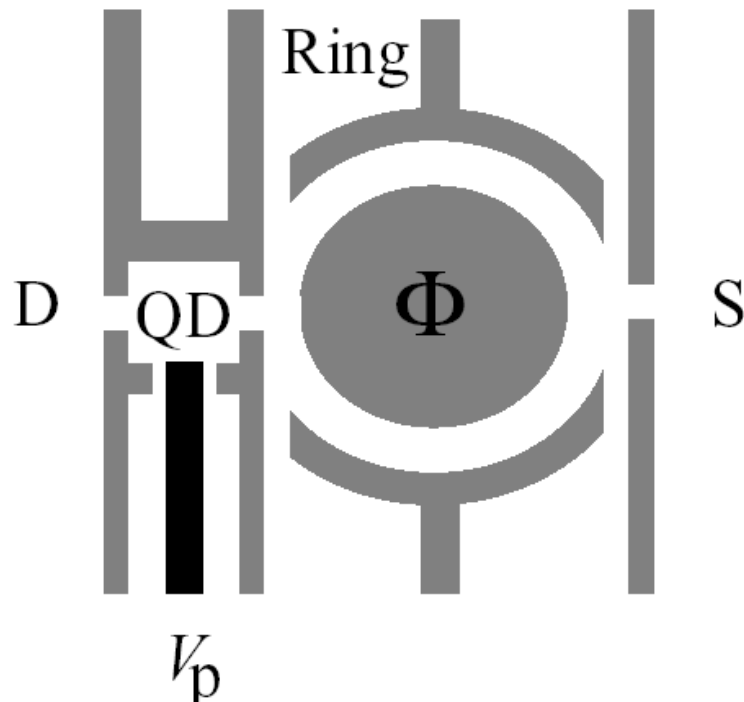
A-B Ring in Semiconductor

# A-B Ring Applications



A-B Ring in Metal

# A-B Ring Applications



A-B oscillation in a Ring with a QD connected in series